p38MAPK (Thr180/Tyr182) antibody, and anti-phospho-PKCδ (Tyr311) antibody were purchased from Cell Signaling. Anti-HA (Y-11), anti-PKCδ (C-20), and anti-Fyn (FYN3) antibodies were purchased from Santa Cruz Biotechnology. Anti-FLAG antibody (Anti-FLAG M2 peroxidase conjugate specific antibody) and antitubulin antibody (clone B-5-1-2) were purchased from Sigma. The anti-c-Yes antibody was purchased from Transduction Laboratories. An anti-CDCP1 antibody (ab1377) was purchased from Abcam Ltd. To generate the CDCP1 antibody, anti-CDCP1 and the anti-phospho-CDCP1 (Tyr734) antibody were obtained by rabbit immunization using the cytoplasmic domain of CDCP1 fused to GST, and the amino peptides NDSHV(pY^{734})AVIEC of CDCP1 were obtained from MBL Co., Ltd. Horseradish peroxidase (HRP)-conjugated anti-mouse and anti-rabbit antibodies were purchased from Amersham Pharmacia. The HRP-conjugated anti-goat immunoglobulin G (IgG) antibody was purchased from ZYMED. Mouse, rabbit, and goat IgGs were purchased from DakoCytomation. The SFK inhibitor PP2 and the structural analog PP3 were purchased from Calbiochem-Novabiochem Ltd. Etoposide and Rottlerin were purchased from Sigma-Aldrich.

Cell culture and transfection. The human lung adenocarcinoma cell lines A549, PC14, and H322 and human lung squamous carcinoma cell lines H520 and H157 were maintained in RPMI 1640 medium with 10% fetal bovine serum (FBS) at 37°C with 5% CO_2. For transfection, cells were seeded on a cell culture plate or a 2-methacryloyloxyethyl phosphorylcholine (MPC)-coated plate (Nunc) at 1.5×10^5 cells per six wells or 9.0×10^5 cells/10-cm plate, and transfection was performed after 14 h. Expression plasmids were transfected by Lipofectamine 2000 (Invitrogen) according to the manufacturer's instructions. To investigate the effect of PP2 treatment, cells were treated with 10 μM of PP2 or 10 μM of PP3.

Construction of dicer, stealth siRNAs, and miR RNAi vectors. Dicer small interfering RNAs (siRNAs) of human c-Src, Fyn, and c-Yes were generated using the BLOCK-iT RNAi TOPO transcription kit and BLOCK-iT complete dicer RNAi kit (Invitrogen) according to the manufacturer's instructions. In the generation of siRNA for Src, a 726-bp fragment from the initiation codon of human c-Src was chosen as the target sequence and amplified by PCR using the primers forward, 5′-ATGGGTAGCAACAAGAGCAAG-3′, and reverse, 5′-GTGGCACAGGCCATCGGCGTG-3′. As for Fyn and c-Yes, 999-bp and 857-bp fragments were chosen as the target sequences, respectively, and amplified with the following primers: Fyn forward, 5′-ATGGGCTGTGTGCAATGTAGG-3′, and reverse, 5′-CACCACTGCATAGAGCTGGAC-3′; c-Yes forward, 5′-CTGAAAATACTCCAGAGCCTG-3′, and reverse, 5′-CTTTGTCCTAGTTTAACCTCTAG-3′. Dicer siRNA of LacZ was generated by the same procedure as dicer siRNAs of c-Src, Fyn, and c-Yes and was used as a negative control. The stealth siRNAs of human CDCP1, PKCδ, and the negative control were ordered from Invitrogen. Specific primers were as follows: CDCP1 forward, 5′-GCUCUGCCACGAGAAAGCAACAUUA-3′, and reverse, 5′-UAAUGUUGCUUUCUCGUGGCAGAGC-3′; PKCδ forward, 5′-GGUGCAGAAGAAGCCGACCAUGUAU-3′, and reverse, 5′-AUACAUGGUCGGCUUCUUCUGCACC-3′. Transfection of both dicer and stealth siRNAs was performed with Lipofectamine 2000 (Invitrogen), and the effect was analyzed less than 48 h after the transfection.

A system stably expressing siRNA was generated using the BLOCK-iT Pol II miR RNAi expression vector kit (Invitrogen) according to the manufacturer's instructions. In the generation of the miR RNAi vector for humans, CDCP1 was chosen as the target sequence, using the forward primer 5′-TGCTGAATGTTGCTTTCTCGTGGCAGGTTTTGGCCACTGACTGACCTGCCACGAAAGCAACATT-3′ and the reverse primer 5′-CCTGAATGTTGCTTTCGTGGCAGGTCAGTCAGTGGCCAAAACCTGCCACGAGAAAGCAACATTC-3′. Cells stably expressing the miR RNAi vector for CDCP1 and LacZ were established and cultured in medium containing blasticidin (Invivogen) at a concentration of 10 μg/ml for 3 weeks. Two clones expressing the CDCP1 RNAi vector (miCDCP1-1 and -2) were selected by significant suppression of the CDCP1 protein (<10%), and two clones from the control LacZ vector were also selected (miLacZ-1 and -2).

Soft-agar colony assay. Six-well tissue culture plates were coated with a layer of RPMI 1640-10% FBS containing 0.5% ultrapure agarose (Invitrogen). Subconfluent A549 cells transfected with the dicer siRNA or miR RNAi vector-expressed clone were treated with EDTA, washed in phosphate-buffered saline twice, and resuspended in RPMI 1640-10% FBS at 6×10^3 cells/ml. Then, a 500-μl cell sample was added to 1 ml of RPMI 1640-10% FBS containing 0.5% ultrapure agarose (final concentration, 0.33%). The cells were plated on the coated tissue culture plates, allowed to solidify, and then placed in a 37°C incubator. After 30 days, colonies were scanned using a GS-800 calibrated densitometer (Bio-Rad), and the numbers of colonies per well were determined. Soft-agar assays were performed three times.

Immunoprecipitation and Western blotting. Cell lysates were prepared with protease inhibitors in PLC buffer (10 mM Tris-HCl, pH 7.5, 5 mM EGTA, 150 mM NaCl, 1% Triton X-100, 10% glycerol, 10 μg/ml aprotinin, 1 mM sodium orthovanadate [Na_3VO_4], and 100 μg/ml leupeptin). The protein concentration was measured by BCA protein assay (Pierce). For purification, 1 μg of monoclonal or affinity-purified polyclonal antibody was added to the proteins, which were then incubated with 500 μl (2 mg/ml) of cell lysate for 2 h at 4°C. Next, they were precipitated with protein A- or protein G-agarose for 1 h at 4°C. The immunoprecipitates were extensively washed with PLC buffer and prepared for Western blotting.

For Western blotting, samples were separated on sodium dodecyl sulfate-polyacrylamide gel electrophoresis and transferred to a polyvinylidene difluoride membrane (Immobilon-P; Millipore). After blocking of the membrane with blocking buffer (Blocking One; Nakarai Tesque), the membrane was probed with antibodies for detection. The membrane was further probed with HRP-conjugated anti-mouse, anti-rabbit, or anti-goat IgG (1:4,000) to visualize the reacted antibody.

Images were captured by a molecular imager (GS-800; Bio-Rad), and the density of each smear was quantified using Quantity One software (Bio-Rad).

Identification of CDCP1. Isolated GST-FynSH2 protein coupled with cyanogen bromide (CNBr) was used to purify the 135-kDa and 70-kDa proteins from the A549 cells cultured for 48 h on MPC-coated plates in growth medium. Briefly, ~3×10^7 suspended A549 cells in a total of 400 dishes (10-cm dish; 30 ml culture medium) were collected and lysed in PLC buffer. The cell lysate was rotated for 8 h at 4°C with GST-FynSH2 protein and washed four times using PLC buffer before being eluted with GST-FynSH2-coupled proteins using 8 M urea buffer (8 M urea, 10 mM Tris-HCl, pH 7.4, 150 mM NaCl, 1% Triton X-100). Secondly, the eluted sample was dialyzed three times against a 100-fold volume of dialysis buffer (10 mM Tris-HCl, pH 7.4, 150 mM NaCl, 1 mM Na_3VO_4), and then the sample was affinity purified with antiphosphotyrosine monoclonal antibody (4G10) coupled with CNBr. 4G10-coupled proteins were washed four times using PLC buffer and once using heptyl-glucoside buffer (10 mM Tris-HCl, pH 7.4, 150 mM NaCl, 0.1% heptyl-glucoside). Next, the samples were eluted using 0.1 M phenylphosphate in heptyl-glucoside buffer. The purified 135-kDa and 70-kDa proteins were concentrated, electrophoresed, and blotted onto a ProBlott membrane (Applied Biosystems). After visualization with colloidal gold total-protein stain (Bio-Rad), the isolated 135-kDa and 70-kDa bands were analyzed by mass spectrometry. Four sets of amino acid sequences determined from the 135-kDa band and an amino acid sequence determined from the 70-kDa band indicated that both the 135-kDa and 70-kDa proteins were CDCP1.

Apoptosis assay. Each cell was treated with EDTA, and 1×10^4 cells were reseeded onto normal or MPC-coated 96-well plates. After 24 h, the cells were lysed and used for the detection of apoptosis. Apoptosis levels were determined using a cell death ELISA kit (Roche Molecular Biochemicals), which detects the presence of nucleosomes in the cytoplasm of apoptotic cells. The absorbance of the samples was measured at a wavelength of 405 nm using a microplate reader model 550 (Bio-Rad).

BrdU incorporation assay. Cell proliferation was analyzed with the cell proliferation ELISA BrdU kit according to the manufacturer's instructions (Roche Molecular Biochemicals) based on the measurement of 5-bromo-2′-deoxyuridine (BrdU) incorporation during DNA synthesis of proliferating cells. Briefly, A549 cells were cultured in triplicate for 24 h in 96-well plates (1.0×10^4 cells/well) with or without cell attachment. The cells were subjected to BrdU incorporation for 6 h. The colorimetric change was measured at 450 nm on a microplate reader model 550 (Bio-Rad).

Infection of retroviral constructs. The retroviral vectors PQCXIN (Clontech) and pCMSCVbsd were used to express human CDCP1 (WT) and Y734F with a FLAG tag at the C terminus and full-length cDNA of Fyn kinase with a double HA tag at the C terminus (FynHA), respectively. pCMSCVbsd contains the blasticidin resistance gene in place of the puromycin resistance gene of pCMSCVpuro (20). These retrovirus vectors were converted into the destination vectors with a vector conversion kit (Invitrogen). The cDNA segments were first cloned into pDONR221 and then into the destination vector, pDEST-PQCXIN or pDEST-CMSCVbsd, according to the manufacturer's instructions (Invitrogen). The production of recombinant retroviruses was performed as described previously (25). Briefly, the retroviral vector and the packaging construct pCL-10A1 were cotransfected into 293T cells using TransIT-293 (Mirus Co., Madison, WI) according to the manufacturer's instructions, and culture fluid was harvested 48 to 72 h posttransfection. H322 cells were infected with the viral fluid in the presence of 4 mg/ml Polybrene, and the infected cells were selected in the presence of 800 μg/ml G418 or 5 μg/ml blasticidin. For combinations of retroviral infections, cells were first transduced with CDCP1 and then with Fyn kinase.

Experimental metastasis assay. Female BALB/cAJcl-nu/nu nude mice were purchased from CLEA Japan Inc. All of the mice used in these experiments were

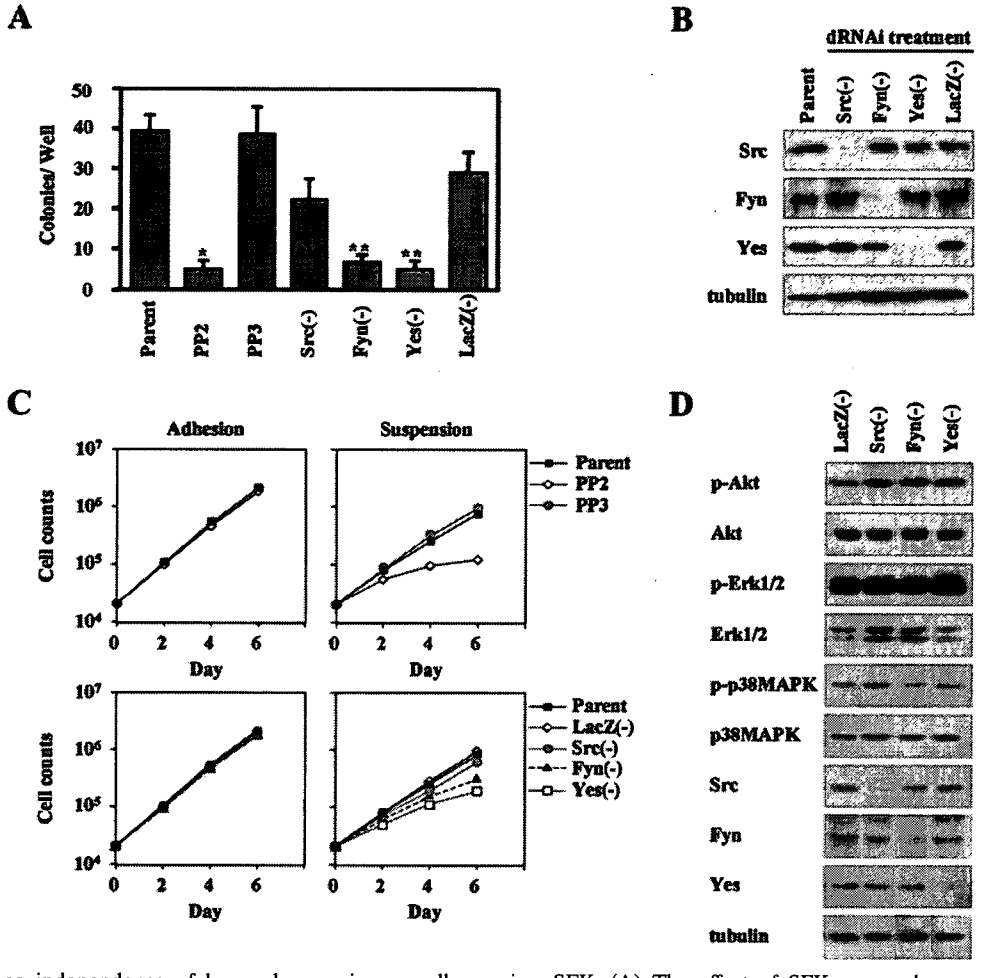

FIG. 1. Anchorage independence of lung adenocarcinoma cells requires SFK. (A) The effect of SFKs on anchorage independence was determined by soft-agar assay. A549 cells were treated with the SFK inhibitor PP2 (10 μM) and SFK dicer RNAi [bars Src(−), Fyn(−), and Yes(−)], and controls [bars Parent, PP3, and LacZ(−)] were seeded onto each soft-agar plate (3×10^3 cells). Colonies equal to and larger than 0.5 mm in diameter were counted after 30 days. The error bars represent standard deviations, and the asterisk indicates statistically significant differences ($P < 0.01$) between the parent and PP2 treatment cells, while the double asterisk indicates statistically significant differences ($P < 0.01$) between LacZ(−) and each of the SFK RNAi treatment cells. (B) A549 cells transiently transfected with c-Src, Fyn, c-Yes, or LacZ dicer RNAi (dRNAi) were incubated for 48 h in culture plates. The cells were lysed and subjected to immunoblotting with the indicated antibodies. (C) Cell growth in A549 cells was subjected to a determination of the number of cells, as described for panel A. Approximately 2×10^4 cells were seeded onto normal (Adhesion) or MPC-coated (Suspension) culture plates with medium. The growth medium was changed every 2 days. The total cell number on each plate was determined every 2 days by a Coulter particle counter z1 (Beckman). (D) SFKs did not affect the phosphorylation of Akt, Erk1/2, or p38MAPK. The lysate of suspended A549 cells transiently transfected with dicer RNAi for each of the SFKs was prepared and subjected to immunoblotting with the indicated antibodies.

6 to 8 weeks old. A549 clones generated by the miR RNAi system and H322 cells were evaluated by experimental metastasis assay, as described by Fidler et al. (8). Briefly, cells (5×10^5 cells/0.2 ml of medium without serum; $n = 6$) were injected into the tail veins of mice. The mice were sacrificed 100 days after cell inoculation for the counting of metastatic nodules. The numbers of lung metastases and nodule formations were determined.

To determine the effect of CDCP1 on tumor growth in nude mice, A549 clones (3×10^6 cells/0.2 ml of medium without serum) were subcutaneously injected into the right flanks of mice. The mice were killed at 30 days. The results are expressed as the mean weight of tumors from three mice ± standard error.

RESULTS

The anchorage independence of lung cancer cells involves SFKs. We first examined the involvement of SFKs in the anchorage independence of A549 lung adenocarcinoma cells using the colony formation assay on soft agar with or without PP2, an SFK inhibitor (Fig. 1A). A549 cells and cells treated with PP3, an inactive derivative of PP2, formed a similar number of colonies in soft agar, while the addition of PP2 caused a significant decrease in the numbers of colonies. A similar effect of PP2 was observed in most lung cancer cells, such as the PC3, PC14, H520, and LK2 cell lines (data not shown).

To determine which member of the SFKs mainly contributes to the anchorage independence of A549 cells, individual expression of c-Src, Fyn, and c-Yes was downregulated using RNAi technology (Fig. 1B), and colony formation assays were performed on soft agar (Fig. 1A). A549 cells treated with Fyn or c-Yes siRNAs formed significantly fewer colonies than the control cells treated with LacZ siRNA, while cells treated with c-Src siRNA formed slightly fewer colonies. We also observed

a similar suppressive effect of Fyn and c-Yes RNAi in PC14 and H520 lung cancer cells (data not shown).

To further assess the significance of SFKs during the anchorage-independent growth, the effects of PP2 or RNAi for each SFK on cell growth were examined with or without cell attachment using a normal culture dish or MPC-coated dish, respectively. In adherent culture, no significant effect on cell numbers was observed by treatment with PP2 or by any siRNA for the SFKs (Fig. 1C, Adhesion). In suspension culture, however, A549 cells treated with PP2 or with siRNAs for Fyn or c-Yes showed a significant reduction of cell counts compared with untreated cells, while cells treated with c-Src siRNA showed only a slight reduction in cell numbers (Fig. 1C, Suspension). Neither control siRNA nor PP3 had a detectable effect on cell growth in suspension culture.

The phosphatidylinositol (PI) 3-kinase/Akt pathway and the MAPK pathway are the most significant pathways mediating growth factor signals during cell survival and cell proliferation. We therefore examined whether downstream signals of SFKs, which lead to anchorage independence of A549 cells, involve the activation of these two pathways. Suppression of the expression of c-Src, Fyn, or c-Yes by each RNAi had no significant effects on the phosphorylation of Akt and ERK in the suspension culture of A549 cells. These sets of siRNAs also had no effect on the phosphorylation of p38MAPK (Fig. 1D).

Taken together, these data suggest that Fyn and c-Yes are required for anchorage independence in A549 cells, and the cellular signals mediated by these kinases are independent of the Akt, ERK, and p38MAPK pathways.

Purification of 135-kDa and 70-kDa phosphotyrosine proteins associating with SFKs in suspension culture. To identify which molecules mediate the SFK signals specific for anchorage independence, we analyzed the phosphotyrosine-containing proteins that bind to SFKs. Among the proteins associated with SFKs, two proteins with molecular masses of 135 kDa and 70 kDa were prominently phosphorylated, even in suspension culture (Fig. 2A), and these proteins were also phosphorylated in PC14 and H520 cell lines, which also exhibit a high level of anchorage independence (Fig. 2A, High). In contrast, the H322 and H157 cell lines, which formed a small number of colonies in soft agar (Fig. 2A, Low), displayed rather lower levels of phosphorylation of these two proteins (Fig. 2A). Using these results, we sought to identify proteins that function as downstream mediators of SFKs in anchorage-independent growth.

As several antibodies against the known phosphoproteins failed to recognize the 135-kDa and 70-kDa proteins, we applied affinity purification. Using A549 cells cultured for 48 h with and without cell attachment, these 135-kDa and 70-kDa proteins were pulled down with the Fyn SH2 domain more efficiently under suspension conditions (Fig. 2B). A total of $\sim 1.2 \times 10^{10}$ cells in suspension culture were first purified with the Fyn SH2 domain. After purification by a second affinity column using a 4G10 antiphosphotyrosine antibody, samples were analyzed by Western blotting (Fig. 2C, WB) and colloidal gold total-protein stain (Fig. 2C, G). Bands corresponding to the two proteins were cut out and analyzed by mass spectrometry. Four peptides from the 135-kDa band and one peptide from the 70-kDa band were determined by mass spectrometry to be the recently identified membrane protein CDCP1 (Fig. 2C). The proteins at molecular masses of both 135 kDa and 70 kDa in the suspension culture appeared to contain the single protein CDCP1. The 70-kDa protein was estimated to be a cleaved product of 135-kDa CDCP1, as previously reported (5).

Identification of the major phosphoprotein of the 135-kDa and 70-kDa proteins as CDCP1 and its association with anchorage independence. Anti-CDCP1 antibody recognized proteins of exactly the same molecular masses as the 135-kDa and 70-kDa proteins both in the whole-cell lysate and in the sample pulled down by the Fyn SH2 domain (Fig. 3A, WCL and PD). CDCP1 was also clearly coimmunoprecipitated with each SFK molecule originally expressed in A549 cells, especially with Fyn and c-Yes, which is consistent with the original 135-kDa protein (Fig. 3A, IP). On the other hand, immunoprecipitation with anti-CDCP1 antibody revealed that CDCP1 was strongly associated with Fyn and c-Yes and very weakly with c-Src (Fig. 3B).

To confirm that the phosphorylation of CDCP1 in each lung cancer cell line is associated with high anchorage independence, we generated a phosphospecific antibody (p-CDCP1 [Tyr734]) against tyrosine 734 of CDCP1, which is reported to be a major phosphorylation site for SFK (1, 5), and analyzed the phosphorylation of CDCP1 in each cell line (Fig. 3C). Prominent phosphorylation of CDCP1 was observed in the A549, PC14, and H520 lung cancer cells with high anchorage independence (Fig. 3C, High), while the H322 and H157 cells, which have low anchorage independence (Fig. 3C, Low), exhibited rather low levels of phosphorylation of CDCP1. From these results, we concluded that the 135-kDa phosphoprotein detected in lung cancer cells is CDCP1, and its phosphorylation status appears to be associated with anchorage independence.

We examined whether the phosphorylation of CDCP1 is altered with or without cell attachment in the culture. After detachment of A549 cells with EDTA, the cells were either plated on a normal dish to cause readhesion or plated on an MPC-coated dish to grow in suspension for 48 h. Under either plating condition, the phosphorylation level of CDCP1 was continuously increased until 24 h; however, it exhibited a sudden decrease at 48 h in adhesion culture, while it increased further in suspension culture (Fig. 3D). Notably, these dynamic changes of phosphorylation during cell suspension and readhesion appear to partially reflect the change in the expression level of CDCP1.

CDCP1 is a regulator of anoikis resistance in lung adenocarcinoma. Next, we checked whether CDCP1 is involved in the regulation of the anchorage independence of A549 cells under the control of SFK activity. For this purpose, we obtained the stable A549 cell clones miCDCP1-1 and miCDCP1-2, which showed suppressed expression of the CDCP1 protein, by using the siRNA for CDCP1 with a BLOCK-iT Pol II miR RNAi expression vector system (Fig. 4A). Both of the clones formed significantly fewer colonies in the soft-agar assay than the LacZ clones (Fig. 4B), suggesting that CDCP1 is actually required for the anchorage independence of A549 lung adenocarcinoma.

Anchorage independence may reflect the persistence of growth and/or survival of cancer cells in suspension; therefore, the effects of CDCP1 expression in suspended cells on cell

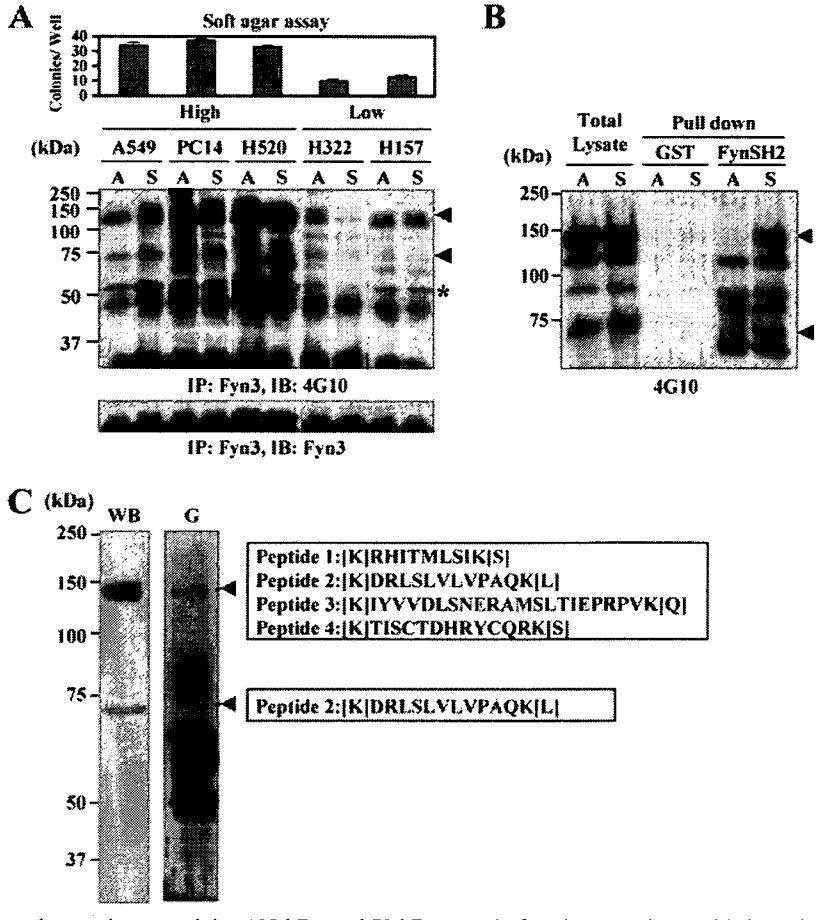

FIG. 2. Purification of phosphotyrosine-containing 135-kDa and 70-kDa protein-forming complexes with SFKs in suspension culture. (A) Anchorage independence in a series of lung cancer cell lines was examined by soft-agar assay (top). The large number of colonies formed in the lung cancer cell lines A549, PC14, and H520 (High) and the small number of colonies formed in the H322 and H157 cell lines (Low) cultured for 48 h under both adhesion and suspension conditions were collected and subjected to immunoprecipitation (IP) with anti-Fyn (Fyn3) antibody and immunoblotting (IB) with antiphosphotyrosine (4G10) antibody. Phosphotyrosine-containing proteins coimmunoprecipitated with Fyn at the molecular masses of 135 kDa and 70 kDa are indicated by arrowheads. The asterisk indicates phosphorylated Fyn. The expression of Fyn in each cell lysate was confirmed by immunoblotting (bottom). A, adhesion; S, suspension. The error bars represent standard deviations. (B) GST-FynSH2 protein generated by *Escherichia coli* was used to pull down the lysate of A549 cells cultured under adhesion or suspension conditions. The isolated samples were immunoblotted with antiphosphotyrosine (4G10) antibody. The arrowheads indicate the phosphotyrosine-containing 135-kDa and 70-kDa proteins. (C) Phosphotyrosine-containing proteins (135 kDa and 70 kDa) were purified according to the protocol described in Materials and Methods. Aliquots of the purified 135-kDa and 70-kDa phosphotyrosine-containing proteins were examined by Western blotting (WB) using antiphosphotyrosine (4G10) antibody, and the remaining samples were stained with colloidal gold total-protein stain (G). Four peptides determined by mass spectrometry (peptides 1 to 4) were identified within the sequence of CDCP1.

proliferation and on cell apoptosis were individually examined. Each miCDCP1 clone in suspension culture showed an increased level of apoptosis compared with miLacZ clones (Fig. 4C). In contrast, no significant change in the cell growth level was observed in each of the miCDCP1 and miLacZ clones compared with the parental A549 cells in suspension culture (Fig. 4D). Importantly, there was no significant change in either cell growth or apoptosis in the adhesion culture (Fig. 4C and D).

We also examined the effect of the expression of phosphorylated CDCP1 on cell proliferation and cell apoptosis using H322 lung adenocarcinoma cells with low anchorage independence. CDCP1 (WT) and/or Fyn kinase with double HA tags at the C terminus (FynHA) were expressed in H322 cells by retroviral vectors, and the expression was checked by Western blotting (Fig. 5A). Additionally, a CDCP1 mutant lacking a putative SFK-binding site (Y734F) was also expressed (2). An increased level of phosphorylation of CDCP1 was observed in H322 cells overexpressing both WT and Fyn kinase (Fig. 5A, WT+FynHA), which caused an inhibition of apoptosis in suspension culture (Fig. 5B). These changes were not observed with either Fyn kinase or WT CDCP1 alone. On the other hand, expression of Y734F alone increased the level of apoptosis in suspension culture, suggesting a dominant-negative effect of this CDCP1 mutant (Fig. 5B, Y734F). A slight enhancement of cell proliferation in suspension culture was observed by expressing Fyn kinase and either WT or mutant CDCP1, but this change was not significant (Fig. 5C).

These results suggest that phosphorylation of CDCP1 confers anchorage independence through the inhibition of apoptosis. In other words, phosphorylation of CDCP1 regulates resistance to anoikis in lung cancer cells.

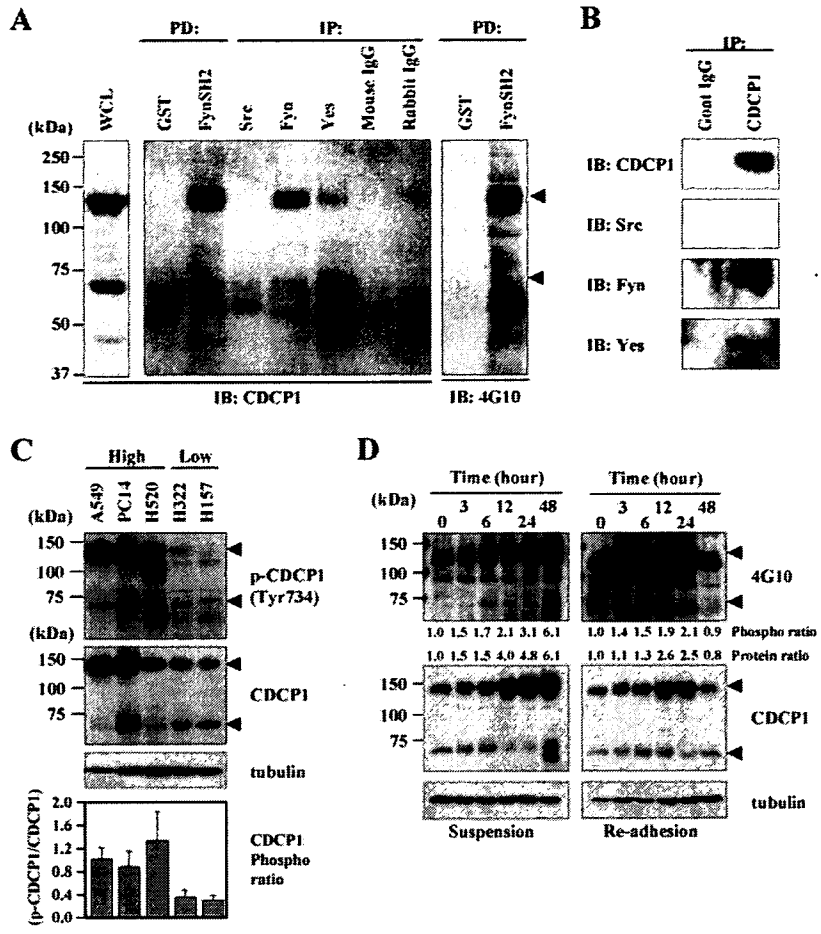

FIG. 3. Identification of the 135-kDa and 70-kDa proteins as CDCP1 and its phosphorylation associated with anchorage independence. (A) The lysate of A549 cells was subjected to whole-cell lysate (WCL) or pull-down assay with GST-FynSH2-protein (PD) or immunoprecipitated with anti-c-Src, anti-Fyn, and anti-c-Yes antibodies (IP) and immunoblotted (IB) with anti-CDCP1 antibody. The same blot was rehybridized with antiphosphotyrosine (4G10) antibody. (B) The lysate of A549 cells was immunoprecipitated with anti-CDCP1 antibody (ab1377) or goat IgG as indicated. The precipitates were subjected to immunoblotting with anti-c-Src, anti-Fyn, anti-c-Yes, and anti-CDCP1 antibodies. (C) The large number of colonies formed by the lung cancer cell lines A549, PC14, and H520 (High) and the small number of colonies formed by the H322 and H157 cell lines (Low) cultured for 48 h in the suspension condition were collected and subjected to immunoblotting with anti-phospho-CDCP1 (Tyr734) and CDCP1 antibodies. This experiment was performed three times. The ratio of the phosphorylation level in each lung adenocarcinoma cell was measured as described in Materials and Methods. The error bars represent standard deviations. (D) Time course analysis of CDCP1 expression and phosphorylation with or without cell attachment. A549 cells were reseeded on normal cell culture plates and an MPC-coated plate at a density of 1.5×10^5 cells per plate with complete medium. For the preparation of the reseeding cells, 2 mM EDTA/Hanks' balanced salt solution was used to detach the cells. For each time point, cells were collected and subjected to immunoblotting with the indicated antibody. The same membrane rehybridized with antitubulin antibody confirmed the concentration of total proteins in each lysate (tubulin). The arrowheads indicate CDCP1.

PKCδ is a signal molecule downstream of CDCP1 during anoikis resistance in lung adenocarcinoma. CDCP1 protein has been shown to bind PKCδ in a phosphorylation-dependent manner (2). PKCδ is a regulator of apoptosis, and it has been reported that the phosphorylation of PKCδ requires the activity of SFKs (37). By treatment with the SFK inhibitor PP2, both the association of PKCδ with CDCP1 and the phosphorylation of PKCδ at Tyr311 were clearly inhibited (Fig. 6A). CDCP1 (WT) and the CDCP1 protein with a point mutation at Tyr734 (Y734F) were C-terminally FLAG tagged and expressed in COS7 cells. After transfection with each plasmid, the association of the Fyn SH2 domain with WT and Y734F mutants was examined. The Fyn SH2 domain was able to pull down the WT but not the Y734F mutants (Fig. 6B, PD: Fyn SH2). The levels of tyrosine phosphorylation of Y734F mutants was much lower than that of the WT in A549 cells (Fig. 6B, IB: 4G10), suggesting that Tyr734 of CDCP1 directly binds to Fyn and that the association is essential for the phosphorylation of CDCP1. The association between CDCP1 and PKCδ was also impaired in the Y734F mutant compared with the WT, indicating that the phosphorylation of CDCP1 is required for the association.

Overexpression of Y734F in A549 cells also blocked the association between PKCδ and CDCP1 and the phosphorylation of PKCδ at Tyr311 (Fig. 6B). Moreover, treatment with CDCP1 siRNA also decreased the phosphorylation level of PKCδ (Fig. 6C). In addition, the phosphorylation level of PKCδ at Tyr311 was elevated in H322 cells by overexpressing both WT CDCP1 and Fyn kinase but not significantly with either the WT, the Y734F mutant, or Fyn kinase alone (see the

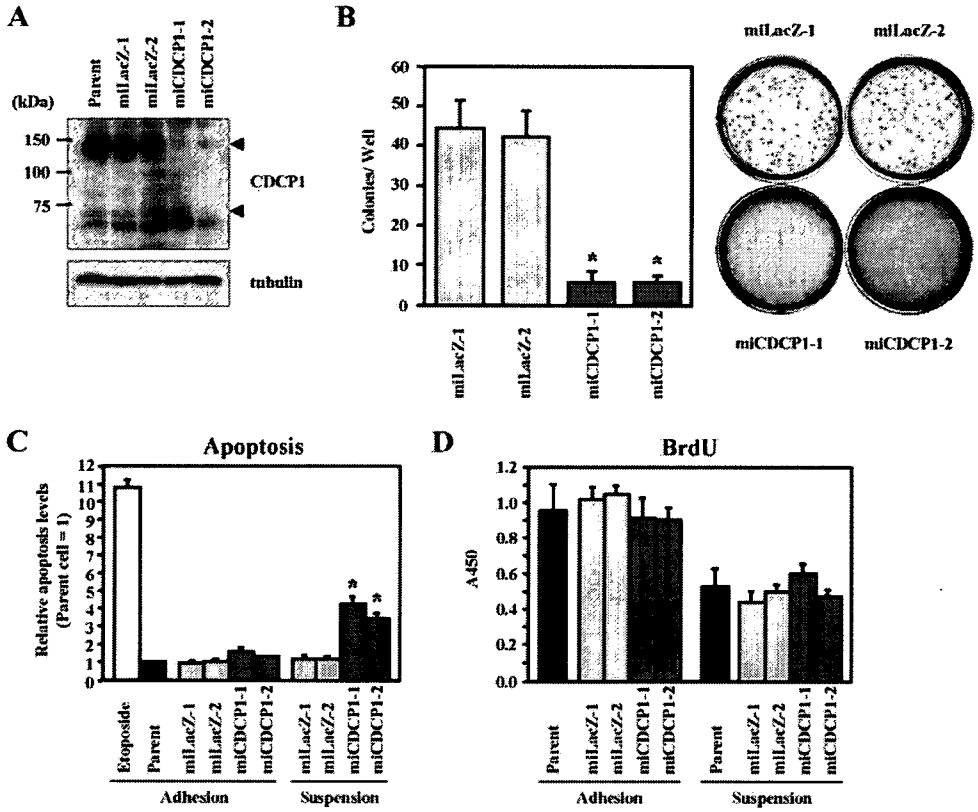

FIG. 4. CDCP1 confers anchorage independence by inhibiting apoptosis in suspended lung adenocarcinoma. (A) CDCP1-defective A549 cell clones (miCDCP1-1 and miCDCP1-2) were generated by an miR RNAi expression vector kit (Invitrogen). miLacZ-1 and miLacZ-2 were control clones. The expression of CDCP1 in each clone (1.5×10^5 cells) cultured for 24 h in an MPC-coated plate was examined by Western blotting using CDCP1 antibody. The concentration of total protein in each clone was confirmed by the same membrane rehybridized with antitubulin antibody (bottom). The arrowheads indicate CDCP1. (B) Each CDCP1-defective clone and control clone was seeded onto soft-agar plates (3×10^3 cells) (right). Colonies equal to and larger than 0.5 mm in diameter were counted after 30 days. The error bars represent standard deviations, and the asterisks indicate statistically significant differences ($P < 0.01$) (left). (C) CDCP1-defective A549 cell clones (miCDCP1-1 and -2) and control miLacZ clones (1.0×10^4 cells) were cultured in normal and MPC-coated 96-well plates. After 24 h, the cells were lysed and apoptosis was examined using a cell death ELISA kit (Roche). The total apoptotic level of A549 cells was examined by treatment with etoposide (25 μM). The relative apoptosis levels are shown as the levels of apoptosis in each clone compared with those of parental cells. In suspension culture, miCDCP1 clones exhibited an increased level of apoptosis compared with that of miLacZ clones. The error bars represent standard deviations, and the asterisks indicate statistically significant differences ($P < 0.01$). (D) Cell proliferation was determined with a cell proliferation ELISA BrdU kit (Roche). Each clone (1.0×10^4 cells) was cultured on normal and MPC-coated 96-well plates. No significant change in cell proliferation was observed in the miCDCP1 or in miLacZ clones compared with parental A549 cells with or without cell attachment. The error bars represent standard deviations.

supplemental material). Therefore, CDCP1 might be required for the phosphorylation of PKCδ by linking PKCδ to SFKs in a phosphorylation-dependent manner.

To check whether PKCδ can regulate anoikis in lung adenocarcinoma cells, cell apoptosis caused by the suspension of miCDCP1 and miLacZ clones was examined with or without PKCδ RNAi. As shown in Fig. 6D, PKCδ RNAi increased the level of apoptosis in the control A549 cells (miLacZ) to a degree similar to that achieved by the suppression of CDCP1 expression (miCDCP1); however, no additive effect on cell apoptosis was observed by the suppression of both CDCP1 and PKCδ. Similar results were obtained from two other independent sets of siRNAs for PKCδ (data not shown). Moreover, treatment with the PKC inhibitor Rottlerin increased the level of apoptosis compared with the parental A549 cells (Fig. 6E). We also examined whether the blocking of the CDCP1-PKCδ signal pathway affects anoikis resistance in A549 cells by overexpressing the C2 domain of PKCδ, which has been shown to be responsible for the association with tyrosine-phosphorylated CDCP1 (2). The HA-tagged C2 domain of PKCδ (C2HA) expressed in A549 cells was actually associated with phosphorylated CDCP1 (Fig. 6F, upper panel) and suppressed the tyrosine phosphorylation levels of PKCδ (Fig. 6F, bottom). At the same time, overexpression of C2HA resulted in a significant increase in the level of apoptosis in suspension culture compared with a mock-transfected control, while it had no significant effect on adherent culture (Fig. 6G).

These results suggest that the CDCP1-SFK complex is required for the phosphorylation of PKCδ under suspension conditions and that PKCδ is a signal molecule for regulating anoikis resistance downstream of CDCP1 signaling.

CDCP1 affects the metastatic potential of A549 lung adenocarcinoma in vivo. Anchorage independence is thought to be an important characteristic of cancer cells that acquire metastatic potential. In order to determine the effect of CDCP1 for in vivo metastasis, miCDCP1 and miLacZ cells were injected

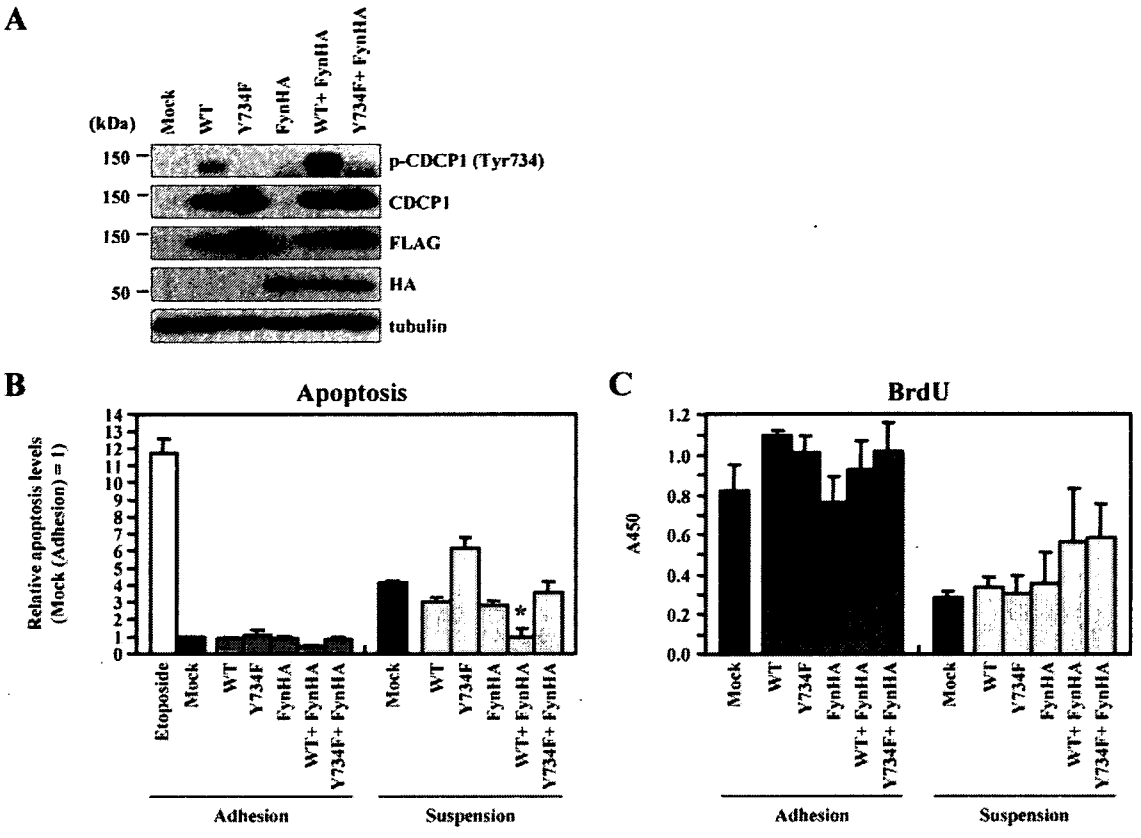

FIG. 5. Anoikis resistance was recovered by phosphorylated CDCP1 in H322 cells with low anchorage independence. (A) H322 cells that overexpressed CDCP1 (WT), a CDCP1 mutant (Y734F), and/or Fyn kinase tagged with HA (FynHA) was incubated for 24 h in MPC-coated plates. The cells were lysed and subjected to immunoblotting with the indicated antibodies. (B) Cells, as indicated (1.0×10^4 cells), were cultured in normal and MPC-coated 96-well plates. After 24 h, the cells were lysed and apoptosis was examined using a cell death ELISA kit (Roche). The total apoptotic level of mock-infected cells was examined by treatment with etoposide (25 μM). The relative apoptosis levels are shown as the levels of apoptosis in each of the cells compared with mock-infected cells in adhesion culture. The error bars represent standard deviations, and the asterisk indicates a statistically significant difference ($P < 0.05$) between mock-transfected cells and other cells in suspension culture. (C) Cell proliferation was determined with a cell proliferation ELISA BrdU kit (Roche). Each of the cells (1.0×10^4 cells) was cultured on normal and MPC-coated 96-well plates. No significant change in cell proliferation was observed in each of the cells compared with mock-infected cells with or without cell attachment (BrdU). The error bars represent standard deviations.

into the tail veins of mice and raised for 100 days. The metastatic capacity was assessed from the number of metastatic cell nodules in mouse lungs. The frequency and number of the metastatic nodules observed in the lungs of each miCDCP1 clone were much less than those found in A549 miLacZ (Fig. 7B). Additionally, H322 cells that belong to the group with low anchorage independence displayed metastasis in only one out of six mice. The average of each of the metastatic nodules and the results of metastasis for each mouse are shown in Table 1. Interestingly, no significant change in tumor growth in nude mice was observed in the miCDCP1-1 clone compared with the A549 miLacZ-1 clone (Fig. 7A). Since the metastatic assay mimics only the middle and late processes of metastasis, these results indicate that CDCP1 affects the later process in the metastasis of lung adenocarcinoma in vivo, possibly through the regulation of anchorage independence.

DISCUSSION

This study has identified CDCP1 as a crucial regulatory molecule of anoikis resistance in lung cancer cells. The signal mediated by the CDCP1-SFK complex appears to play the principal role in overcoming anoikis. CDCP1 has previously been identified as a novel epithelial tumor antigen (28) and as a tumor-associated protein preferentially expressed by highly metastatic epidermoid carcinoma (15), although little is known about the function of CDCP1 in tumor cells. Some putative functions have been suggested, such as the hypothesis that CDCP1 is a mitotic substrate of SFKs under cell cycle regulation in MDA-468 breast cancer cells (3). In this study, we found a distinct novel function of CDCP1 in tumor cells that occurs through phosphorylation by SFKs.

We found that the disruption of CDCP1 expression in A549 cells resulted in defective colony formation in soft agar, suggesting that CDCP1 affects anchorage independence (Fig. 4B). Anchorage independence is an outstanding characteristic of tumor cells, which confers the ability to grow without attachment to the extracellular matrix. Anchorage independence may come from either persistent cell growth or resistance to apoptosis in a suspension condition. As found in this study, CDCP1 does not significantly affect cell growth. A key finding here is that the loss of CDCP1 induces the apoptosis of lung

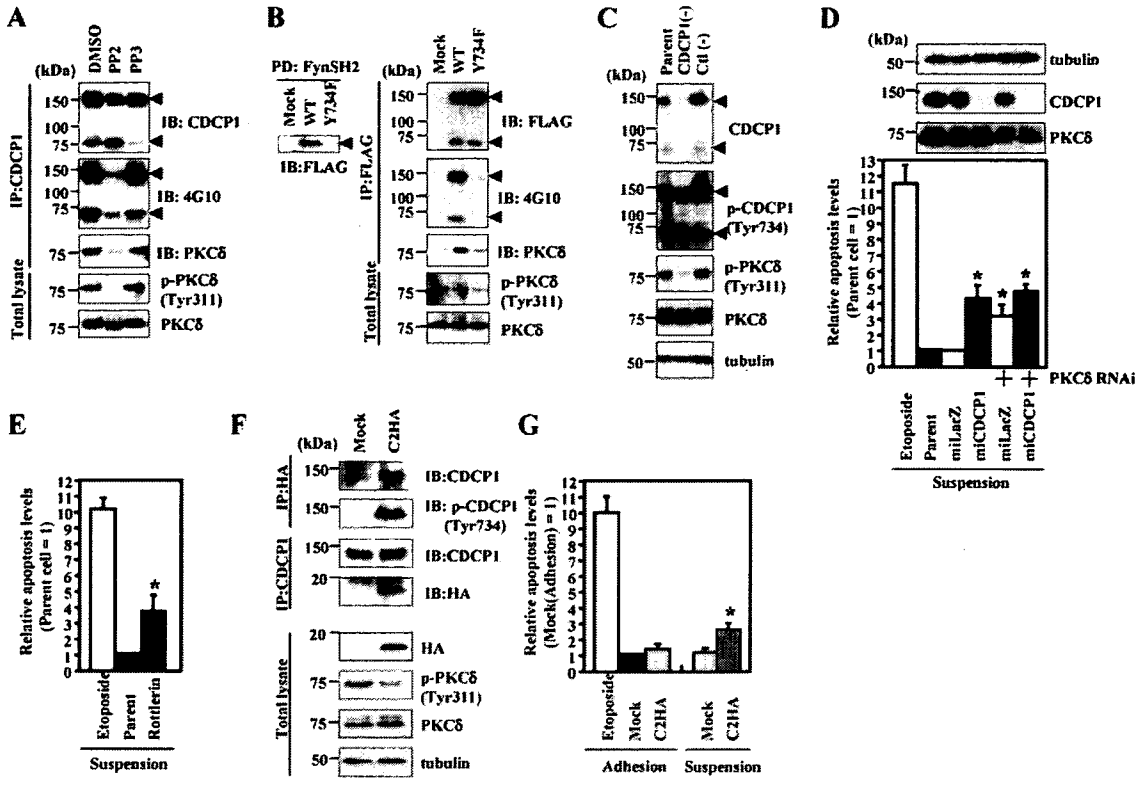

FIG. 6. PKCδ is a signaling molecule downstream of CDCP1 during anoikis resistance. (A) Treatment with the SFK inhibitor PP2 blocked the physical association between PKCδ and CDCP1 and at the same time suppressed phosphorylation of PKCδ at Tyr311. A549 cells treated with 10 μM of PP2 and 10 μM of PP3 in suspension culture were collected and subjected to immunoprecipitation with anti-CDCP1 antibody (ab1377) and immunoblotting (IB) with the indicated antibodies. The phospho-specific antibody against PKCδ (p-PKCδ [Tyr311]) total cell lysate was used to detect the phosphorylation of PKCδ, and the expression of PKCδ was also confirmed. (B) CDCP1 mutants were expressed in COS7 cells and pulled down (PD) with GST-FynSH2 protein. The samples pulled down were immunoblotted with FLAGM2 antibody (left). CDCP1 mutants were transiently transfected in A549 cells. After 24 h, cells were collected and subjected to immunoprecipitation (IP) with anti-FLAGM2 antibody. The immunoprecipitates were subjected to immunoblotting with the indicated antibodies. Each total cell lysate was used to detect the phosphorylation and the expression of PKCδ. (C) A549 cells treated with CDCP1 stealth siRNA and control siRNA were collected and subjected to immunoblotting with the indicated antibodies. (D) The effect of PKCδ on apoptosis was determined by apoptosis assay. PKCδ stealth siRNA was transiently transfected into CDCP1-defective A549 cell clones and control miLacZ clones. After 48 h, each cell clone (1.0×10^4 cells) was reseeded onto MPC-coated 96-well plates and cultured for 24 h. The cells were lysed and examined for apoptosis using a cell death ELISA kit (Roche). The total apoptotic level of A549 cells was examined by treatment with etoposide (25 μM). The relative apoptosis levels are shown as the level of apoptosis compared with the parent cells. The error bars represent standard deviations, and the asterisks indicate statistically significant differences ($P < 0.01$) between the parent and each of the other cells. Expression of CDCP1 and PKCδ was determined by Western blotting with the indicated antibodies (top). (E) The effect of PKCδ activation on apoptosis was determined by apoptosis assay. A549 cells (1.0×10^4 cells) were seeded onto MPC-coated 96-well plates and treated or not with Rottlerin (5 μM). The relative apoptosis levels after culture for 24 h are shown as the level of apoptosis compared with parent cells. The error bars represent standard deviations, and the asterisk indicates a statistically significant difference ($P < 0.01$) between the parent and Rottlerin-treated cells. (F) The C2 domain of PKCδ with the HA tag (C2HA) was expressed in A549 cells. After 24 h, cells were collected and subjected to immunoprecipitation with anti-CDCP1 (ab1377) or anti-HA antibody. Immunoprecipitates were subjected to immunoblotting with the indicated antibodies. Total cell lysate was used to detect the expression of C2HA and the phosphorylation level of endogenous PKCδ in A549 cells. (G) The cells transiently transfected with C2HA or mock vector, as indicated (1.0×10^4 cells), were cultured in normal and MPC-coated 96-well plates. After 24 h, the cells were lysed and apoptosis was examined using a cell death ELISA kit (Roche). The relative apoptosis levels are shown as the level of apoptosis in each of the cells compared with the control mock cells in adhesion culture. The error bars represent standard deviations, and the asterisk indicates a statistically significant difference ($P < 0.05$) between the mock cells and each of the other cells in suspension culture.

adenocarcinoma cells in a suspended condition but not in an adherent condition (Fig. 4C). This phenomenon strongly suggests that CDCP1 is involved in the suppression of anoikis, a form of apoptosis triggered by disruption of cell-matrix interactions.

The molecules and signaling pathways in the anoikis resistance of human cancer cells are not sufficiently understood. Previous reports have shown that oncogenes encoding, e.g., Ras, Src, and their downstream signaling molecules, such as PI 3-kinase/Akt and MAPK, are critical players in compensating for the cell survival signals derived from matrix attachment via integrins (9, 16). Inhibition of PI 3-kinase/Akt and Erk1/2 does not induce apoptosis in lung cancer cells, while SFK inhibitor causes apoptosis in these cells (32, 33). This study has revealed that the inhibition of SFKs blocked anchorage independence in lung cancer cells without affecting the phosphorylation state of PI 3-kinase/Akt, Erk1/2, or p38MAPK (Fig. 1D). These results suggest that SFKs are critical regulators of anoikis in cancer cells. On the other hand, the inhibition of SFKs was effected independently of the PI 3-kinase/Akt pathway.

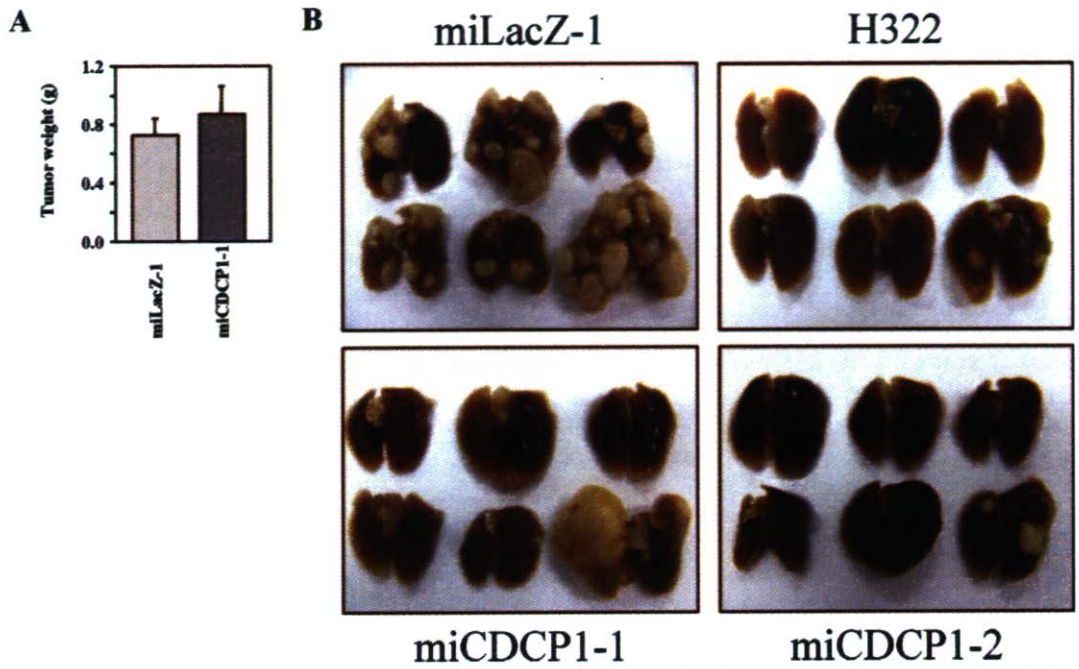

FIG. 7. Metastatic capacity of CDCP1-defective lung adenocarcinoma cells. (A) The effect of CDCP1 on tumor growth in nude mice was determined as described in Materials and Methods. The data represent the weights of tumors from the miCDCP1-1 clone or the miLacZ-1 clone (n = 3). The error bars indicate standard deviations. (B) The metastatic potential was evaluated from the number of metastatic cell nodules in mouse lungs after injection of tumor cells from the tail vein (n = 6). Lung tissues were fixed with 10% formaldehyde solution. Many metastatic nodules were observed in the control A549 miLacZ-1 clone, while fewer nodules were observed in the miCDCP1-1 and miCDCP1-2 clones and H322 cells. The number of mice with obvious lung metastasis and the average number of metastatic nodules per mouse for each cell clone are shown in Table 1.

CDCP1 is a potent substrate of SFKs within cells, and its function is likely modulated by phosphorylation of the tyrosine residues in the cytoplasmic domain (2, 3, 5). In our study, the SFK inhibitor PP2 inhibited phosphorylation of CDCP1, and at the same time, soft-agar colony formation of A549 cells was also inhibited (Fig. 1A, PP2). In fact, the level of tyrosine phosphorylation of CDCP1 is associated with the capacity for anchorage independence in lung cancer cells (Fig. 3C). Together with the observation that apoptosis of H322 cells in suspension culture was inhibited by overexpression of CDCP1 and Fyn kinase together but not CDCP1 or Fyn kinase alone, or by the Y734F mutant of CDCP1, this suggested that active SFKs confer anoikis resistance through tyrosine phosphorylation of CDCP1.

Among the SFKs, the expression of c-Src, Fyn, and c-Yes is commonly observed in human solid tumors (31). In this study, we detected the expression of c-Src, Fyn, and c-Yes in the suspension culture of A549 cells (Fig. 1B, Parent). Among these kinases, Fyn and c-Yes may regulate CDCP1-mediated cell survival in A549 cells, since these kinases are associated with CDCP1 (Fig. 3A and B), and downregulation of Fyn or c-Yes inhibits soft-agar colony formation in A549 cells (Fig. 1A). On the other hand, the amount of phosphorylated CDCP1 was either partially or remarkably reduced by Fyn or c-Yes dicer siRNA, respectively (data not shown), supporting the claim that these two members of the SFKs have a considerable effect on the phosphorylation of CDCP1. A dynamic balance of active SFK and protein tyrosine phosphatase activities regulates the phosphorylation of CDCP1 during cell attachment (5). This balance may shift when integrin signaling is shut off by cell detachment. As shown in Fig. 3D, dynamic changes in the amount of tyrosine-phosphorylated CDCP1 were also caused by changes in the expression level of CDCP1, although it is not yet clearly understood how the expression of CDCP1 is regulated by the cell detachment/attachment signal.

Benes et al. (2) recently reported that the C2 domain of PKCδ associates with phosphorylated CDCP1. Several studies have also reported on the phosphorylation of PKCδ by SFKs (19, 30), but the regulatory mechanism of PKCδ phosphorylation remains unclear. Our study found that PKCδ was remarkably phosphorylated in suspended A549 cells and also confirmed a physical association through the regulation of the phosphorylation state of CDCP1 in A549 lung adenocarcinoma cells (Fig. 6A, B, and C). Both the expression of CDCP1

TABLE 1. Effects of CDCP1 downregulation on lung cancer metastasis in vivo[a]

Cells	Metastasis[b]	No. of nodules in lung[c]
A549 miLacZ	6/6	12.8
H322	1/6	1.3
A549 miCDCP1-1	1/6	0.2
A549 miCDCP1-2	1/6	0.5

[a] Mice were sacrificed 100 days after inoculation.
[b] Data are shown as the number of mice bearing tumors in the lung/total number of mice.
[c] Average number of metastatic tumor nodules larger than 2 mm in the lung per mouse.

and the association of CDCP1 with SFKs are required for the phosphorylation of PKCδ, which suggests that CDCP1 mediates the phosphorylation of PKCδ by SFKs. We found that an increased level of apoptosis was observed with the treatment of siRNA for PKCδ or with the PKC inhibitor Rottlerin in A549 cells in a suspension condition (Fig. 6D and E). Moreover, inhibition of the association between CDCP1 and PKCδ, by expressing the C2 domain of PKCδ, suppressed the tyrosine phosphorylation of PKCδ and increased the level of apoptosis in A549 cells in a suspension condition at the same time (Fig. 6F and G). It is speculated that CDCP1-mediated tyrosine phosphorylation and the activation of PKCδ lead to the suppression of apoptosis in A549 cells.

Tyrosine phosphorylation of PKCδ is a critical regulatory factor for PKCδ activity and results in the elevation of both tyrosine phosphorylation and the activity of PKCδ in various cells stimulated with substances such as phorbol esters, growth factors, and hormones (21, 22, 23, 27, 29). It was also reported that tyrosine phosphorylation of PKCδ by Src actually increased PKCδ activity (1, 11). On the other hand, several reports have shown that active PKCδ possesses an antiapoptotic function. For example, the activation of PKCδ by fibroblast growth factor has an antiapoptotic effect in PC12 cells (34) and a reduction of PKCδ activity by using a kinase-dead mutant of PKCδ induced apoptosis in lung cancer cells (7). Further evidence that supports PKCδ as a suppressor of apoptosis includes the requirement for active PKCδ during cell transformation mediated by insulin-like growth factor I receptor (23) and the induction of anchorage-independent growth and increased metastatic potential of breast cancer cells overexpressing PKCδ (17, 18). Our observation that tyrosine-phosphorylated PKCδ serves an antiapoptotic function in lung cancer cells supports these reports, although it appears that PKCδ has both proapoptotic and antiapoptotic functions, which are dependent on the specific circumstances and modes of action (4).

Taken together, it is strongly suggested that CDCP1 is a docking protein between SFKs and PKCδ and that CDCP1-SFK complex-dependent PKCδ phosphorylation plays a significant role in the control of anoikis resistance in lung adenocarcinoma cells. Further study is required to identify the signal downstream of tyrosine-phosphorylated PKCδ.

Finally, this study suggests that CDCP1 is a novel regulator of anoikis resistance under the control of SFKs in lung adenocarcinoma cells and that PKCδ, which is associated with and conditionally phosphorylated by the CDCP1-SFK complex, is a good candidate as a signal mediator of anoikis resistance. It was found that CDCP1 is essential in vivo for lung cancer metastasis in the mouse model (Fig. 7), indicating that CDCP1 is actually a modulator of the later processes of cancer metastasis through the regulation of anoikis. Further investigation of the specific functions of CDCP1 in normal cells and its disorders in cancer may yield important information that will help determine a clinical target for lung cancer metastasis.

ACKNOWLEDGMENTS

We thank M. Iigo for technical assistance with the in vivo metastasis model and M. Tanaka for useful discussions (National Cancer Center Research Institute, Tokyo, Japan).

This work was supported by a Grant-in-Aid for Cancer Research and a Grant-in-Aid for Young Scientists by the Ministry of Education, Culture, Sports, Science and Technology of Japan, and in part by a Grant-in-Aid from the Ministry of Health, Labor and Welfare of Japan for the third-term Comprehensive 10-year Strategy for Cancer Control.

REFERENCES

1. **Benes, C., and S. P. Soltoff.** 2001. Modulation of PKCδ tyrosine phosphorylation and activity in salivary and PC-12 cells by Src kinases. Am. J. Physiol. Cell Physiol. **280:**C1498–C1510.
2. **Benes, C. H., N. Wu, A. H. Elia, T. Dharia, L. C. Cantley, and S. P. Soltoff.** 2005. The C2 domain of PKCδ is a phosphotyrosine binding domain. Cell **121:**271–280.
3. **Bhatt, A. S., H. Erdjument-Bromage, P. Tempst, C. S. Craik, and M. M. Moasser.** 2005. Adhesion signaling by a novel mitotic substrate of Src kinases. Oncogene **24:**5333–5343.
4. **Brodie, C., and P. M. Blumberg.** 2003. Regulation of cell apoptosis by protein kinase C δ. Apoptosis **8:**19–27.
5. **Brown, T. A., T. M. Yang, T. Zaitsevskaia, Y. Xia, C. A. Dunn, R. O. Sigle, B. Kundsen, and W. G. Carter.** 2004. Adhesion or plasmin regulates tyrosine phosphorylation of a novel membrane glycoprotein p80/gp140/CUB domain-containing protein 1 in epithelia. J. Biol. Chem. **279:**14772–14783.
6. **Buhring, H. J., S. Kuci, T. Conze, G. Rathke, K. Bartolovic, F. Grunebach, M. Scherl-Mostageer, T. H. Brummendorf, N. Schweifer, and R. Lammers.** 2004. CDCP1 identifies a broad spectrum of normal and malignant stem/progenitor cell subsets of hematopoietic and nonhematopoietic origin. Stem Cells **22:**334–343.
7. **Clark, A. S., K. A. West, P. M. Blumberg, and P. A. Dennis.** 2003. Altered protein kinase C (PKC) isoforms in non-small cell lung cancer cells: PKCδ promotes cellular survival and chemotherapeutic resistance. Cancer Res. **63:**780–786.
8. **Fidler, I. J., E. Gruys, M. A. Cifone, Z. Banes, and C. Bucana.** 1981. Demonstration of multiple phenotypic diversity in a murine melanoma of recent origin. J. Natl. Cancer Inst. **67:**947–956.
9. **Frisch, S. M., and H. Francis.** 1994. Disruption of epithelial cell-matrix interactions induces apoptosis. J. Cell Biol. **124:**619–626.
10. **Frisch, S. M., and R. A. Screaton.** 2001. Anoikis mechanisms. Curr. Opin. Cell Biol. **13:**555–562.
11. **Gschwendt, M., K. Kielbassa, W. Kittstein, and F. Marks.** 1994. Tyrosine phosphorylation and stimulation of protein kinase C δ from porcine spleen by src in vitro. Dependence on the activated state of protein kinase C δ. FEBS Lett. **347:**85–89.
12. **Hanahan, D., and R. A. Weiberg.** 2000. The hallmarks of cancer. Cell **100:** 57–70.
13. **Hisano, C., R. Tanaka, H. Fujishima, H. Ariyama, T. Tsuchiya, T. Tatsumoto, K. Mitsugi, M. Nakamura, and S. Nakano.** 2003. Suppression of anoikis by v-Src but not by activated c-H-ras in human gallbladder epithelial cells. Cell Biol. Int. **27:**415–421.
14. **Ho, S. N., H. D. Hunt, R. M. Horton, J. K. Pullen, and L. R. Pease.** 1989. Site-direct mutagenesis by overlap extension using the polymerase chain reaction. Gene **77:**51–59.
15. **Hooper, J. D., A. Zijlstra, R. T. Aimes, H. Liang, G. F. Claassen, D. Tarin, J. E. Testa, and J. P. Quigley.** 2003. Subtractive immunization using highly metastatic human tumor cells identifies SIMA135/CDCP1, a 135 kDa cell surface phosphorylated glycoprotein antigen. Oncogene **22:**1783–1794.
16. **Khwaja, A., P. Rodriguez-Viciana, S. Wennstrom, P. H. Warne, and J. Downward.** 1997. Matrix adhesion and Ras transformation both activate a phosphoinositide 3-OH kinase and protein kinase B/Akt cellular survival pathway. EMBO J. **16:**2783–2793.
17. **Kiley, S. C., K. J. Clark, S. K. Duddy, R. D. Welch, and S. Jaken.** 1999. Increased protein kinase C δ in mammary tumor cell: relationship to transformation and metastatic progression. Oncogene **18:**6748–6757.
18. **Kiley, S. C., K. J. Clark, M. Goodnough, D. R. Welch, and S. Jaken.** 1999. Protein kinase C δ involvement in mammary tumor cell metastasis. Cancer Res. **59:**3230–3238.
19. **Kronfeld, I., G. Kazimirsky, P. S. Lorenzo, S. H. Garfield, P. M. Blumberg, and C. Brodie.** 2000. Phosphorylation of PKCδ on distinct tyrosine residues regulates specific cellular functions. J. Biol. Chem. **275:**35491–35498.
20. **Kyo, S., M. Nakamura, T. Kiyono, Y. Maida, T. Kanaya, M. Tanaka, N. Yatabe, and M. Inoue.** 2003. Successful immortalization of endometrial glandular cells with normal structural and functional characteristics. Am. J. Pathol. **163:**2259–2269.
21. **Li, W., H. Mischak, J. C. Yu, L. M. Wang, J. F. Mushinski, M. A. Heidaran, and J. H. Pierce.** 1994. Tyrosine phosphorylation of protein kinase C-delta in response to its activation. J. Biol. Chem. **269:**2349–2352.
22. **Li, W., J. C. Yu, P. Michieli, J. F. Beeler, N. Ellmore, M. A. Heidaran, and J. H. Pierce.** 1994. Stimulation of the platelet-derived growth factor beta receptor signaling pathway activates protein kinase C-delta. Mol. Cell. Biol. **14:**6727–6735.
23. **Li, W., Y. X. Jiang, J. Zhang, L. Soon, L. Flechner, V. Kapoor, J. H. Pierce,**

and L. H. Wang. 1998. Protein kinase C-δ is an important signaling molecule in insulin-like growth factor I receptor-mediated cell transformation. Mol. Cell. Biol. **18**:5888–5898.
24. **Michel, J. B.** 2003. Anoikis in the cardiovascular system: known and unknown extracellular mediators. Arterioscler. Thromb. Vasc. Biol. **23**:2146–2154.
25. **Naviaux, R. K., E. Costanzi, M. Haas, and I. M. Verma.** 1996. The pCL vector system: rapid production of helper-free, high-titer, recombinant retroviruses. J. Virol. **70**:5701–5705.
26. **Payford, M. P., and M. D. Schaller.** 2004. The interplay between Src and integrins in normal and tumor biology. Oncogene **23**:7928–7946.
27. **Popoff, I. J., and J. P. Dean.** 1999. Activation and tyrosine phosphorylation of protein kinase C delta in response to B cell antigen receptor stimulation. Mol. Immunol. **36**:1005–1016.
28. **Scherl-Mostageer, M., W. Sommergruber, R. Abseher, R. Hauptmann, P. Ambros, and N. Schweifer.** 2001. Identification of a novel gene, CDCP1, overexpressed in human colorectal cancer. Oncogene **20**:4402–4408.
29. **Soltoff, S. P., and A. Toker.** 1995. Carbachol, substance P, and phorbol ester promote the tyrosine phosphorylation of protein kinase C δ in salivary gland epithelial cells. J. Biol. Chem. **270**:13490–13495.
30. **Song, J. S., P. G. Swann, Z. Szallasi, U. Blank, P. M. Blumberg, and J. Rivera.** 1998. Tyrosine phosphorylation-dependent and -independent associations of protein kinase C-δ with Src family kinase in the RBL-2H3 mast cell line: regulation of Src family kinase activity by protein kinase C-δ. Oncogene **16**:3357–3368.
31. **Summy, J. M., and G. E. Gallick.** 2003. Src family kinases in tumor progression and metastasis. Cancer Metastasis Rev. **22**:337–358.
32. **Wei, L., Y. Yang, and Q. Yu.** 2001. Tyrosine kinase-dependent, phosphatidylinositol 3′-kinase, and mitogen-activated protein kinase-independent signaling pathways prevent lung adenocarcinoma cells from anoikis. Cancer Res. **61**:2439–2444.
33. **Wei, L., Y. Yang, X. Zhang, and Q. Yu.** 2004. Altered regulation of Src upon cell detachment protects human lung adenocarcinoma cells from anoikis. Oncogene **23**:9052–9061.
34. **Wert, M. M., and H. C. Palfrey.** 2000. Divergence in the anti-apoptotic signaling pathways used by nerve growth factor and basic fibroblast growth factor (bFGF) in PC12 cells: rescue by bFGF involves protein kinase Cδ. Biochem. J. **352**:175–182.
35. **Windham, T. C., N. U. Parikh, D. R. Siwak, J. M. Summy, D. J. McConkey, A. J. Kraker, and G. E. Gallick.** 2002. Src activation regulates anoikis in human colon tumor cell lines. Oncogene **21**:7797–7807.
36. **Yeatman, T. J.** 2004. A renaissance for Src. Nat. Rev. Cancer **4**:470–480.
37. **Zhong, M., Z. Lu, and D. A. Foster.** 2002. Downregulation PKCδ provides a PI3K/Akt-independent survival signal that overcomes apoptotic signals generated by c-Src overexpression. Oncogene **21**:1071–1078.

Functional analysis of Src homology 3-encoding exon (exon 2) of p130Cas in primary fibroblasts derived from exon 2-specific knockout mice

Tatsuya Tazaki[1,2], Kazuko Miyazaki[1], Eiso Hiyama[3], Tetsuya Nakamoto[4], Ryuichi Sakai[5], Norimasa Yamasaki[1], Zen-ichiro Honda[6], Masaki Noda[7], Nobuyuki Miyasaka[4], Taijiro Sueda[2] and Hiroaki Honda[1,*]

[1]*Department of Developmental Biology, Research Institute for Radiation Biology and Medicine, Hiroshima University, Hiroshima 734-8553, Japan*

[2]*Department of Surgery, Graduate School of Biomedical Sciences, Hiroshima University, Hiroshima 734-8553, Japan*

[3]*Natural Science Center for Basic Research and Development, Hiroshima University, Hiroshima 734-8553, Japan*

[4]*Department of Medicine and Rheumatology, Tokyo Medical and Dental University, Tokyo, 113-8519, Japan*

[5]*Growth Factor Division, National Cancer Center Research Institute, Tokyo, 104-0045, Japan*

[6]*Department of Allergy and Rheumatology, Faculty of Medicine, Graduate School of Medicine, University of Tokyo, Tokyo 113-8655, Japan*

[7]*Department of Molecular Pharmacology, Medical Research Institute, Tokyo Medical and Dental University, Tokyo, 113-8519, Japan*

p130Cas (Cas, Crk-associated substrate) is an adaptor molecule composed of a Src homology 3 (SH3) domain, a substrate domain (SD) and a Src binding domain (SBD). The SH3 domain of Cas associates with focal adhesion kinase (FAK), but its role in cellular function has not fully been understood. To address this issue, we established and analyzed primary fibroblasts derived from mice expressing a truncated Cas lacking exon 2, which encodes the SH3 domain (Cas Δexon 2). In comparison to wild-type cells, Cas exon $2^{\Delta/\Delta}$ cells showed reduced motility, which could be due to impaired tyrosine-phosphorylation of FAK and Cas, reduced FAK/Cas/Src/CrkII binding, and also impaired localization of Cas Δexon 2 to focal adhesions on fibronectin. In addition, to analyze downstream signaling pathways regulated by Cas exon 2, we performed microarray analyses. Interestingly, we found that a deficiency of Cas exon 2 up-regulated expression of CXC Chemokine Receptor-4 and CC Chemokine Receptor-5, which may be regulated by IκBα phosphorylation. These results indicate that the SH3-encoding exon of Cas participates in cell motility, tyrosine-phosphorylation of FAK and Cas, FAK/Cas/Src/CrkII complex formation, recruitment of Cas to focal adhesions and regulation of cell motility-associated gene expression in primary fibroblasts.

Introduction

Cas is composed of an N-terminal Src homology 3 (SH3) domain, a substrate domain (SD) that consists of a cluster of Tyr-Xaa-Xaa-Pro (YXXP) motifs (one YLVP, four YQXPs, nine YDXPs and one YAVP), a C-terminal Src binding domain (SBD) and other regions (Sakai *et al.* 1994). The SH3 domain binds to the proline-rich region of various signaling molecules, such as focal adhesion kinase (FAK) (Polte & Hanks 1995), PTP-1B (Liu *et al.* 1996), PTP-PEST (Garton *et al.* 1997), C3G (Kirsch *et al.* 1998) and CIZ (Nakamoto *et al.* 2000). The SD offers docking sites for the SH2 domain of several molecules including CrkII, Nck and an inositol 5′-phophatase, SHIP2 (SH2-containing inositol 5-phosphatase) in a tyrosine-phosphorylation-dependent manner (Mayer *et al.* 1995; Schlaepfer *et al.* 1997; Prasad *et al.* 2001). The SBD is rich in proline and serves as a binding site for the SH2 and SH3 domains of Src kinase (Nakamoto *et al.* 1996).

Communicated by: Kohei Miyazono

**Correspondence:* E-mail: hhonda@hiroshima-u.ac.jp

DOI: 10.1111/j.1365-2443.2007.01156.x

Physiologically, Cas becomes tyrosine phosphorylated in response to various extracellular stimuli, such as integrin engagement (Nojima *et al.* 1995; Vuori & Ruoslahti 1995), which recruits Cas from cytoplasm to focal adhesions (Nakamoto *et al.* 1997). Tyrosine-phosphorylated Cas binds to CrkII, forming a Cas/CrkII complex (Vuori *et al.* 1996), which subsequently leads to the activation of the Rac–JNK pathway (Dolfi *et al.* 1998; Kiyokawa *et al.* 1998a). In addition, over-expression of Cas promotes cell motility, depending on its association with FAK and CrkII (Cary *et al.* 1998; Klemke *et al.* 1998).

To clarify biological roles of Cas, we generated Cas-deficient mice (Honda *et al.* 1998). Cas-deficient embryos died *in utero* at 12.5 dpc showing marked systemic congestion and growth retardation (Honda *et al.* 1998). Histologically, the heart was poorly developed and blood vessels were prominently dilated. Electron microscope analysis of the heart revealed disorganization of myofibrils and disruption of Z-disks (Honda *et al.* 1998). Cas-deficient fibroblasts showed impaired actin stress fiber formation, defects in cell migration, delayed cell spreading and resistance to Src-induced transformation (Honda *et al.* 1998, 1999). These results demonstrated that Cas is an actin-assembly molecule, which plays an essential role in embryonic development, cytoskeletal organization and Src-induced cellular transformation. Subsequently, to examine the role of each domain of Cas in these processes, we performed a compensation assay by expressing a series of Cas mutants in Cas-deficient fibroblasts (Huang *et al.* 2002). The results showed that motifs containing YDXP were indispensable for actin cytoskeleton organization and cell migration, suggesting that CrkII-mediated signaling regulates these biological processes (Huang *et al.* 2002). In contrast, C-terminal SBD was essential for cell migration, Src-induced transformation and membrane localization of Cas, but was dispensable for the organization of actin stress fibers (Huang *et al.* 2002). Although the above results provided insights in the roles of SD and SBD, the role of the SH3 domain of Cas, which has been shown to associate with various signaling molecules, remains unclear.

To address this issue, we generated mice deficient in Cas exon 2, which produce a truncated Cas protein lacking the SH3 domain. Heterozygous (Cas exon $2^{+/\Delta}$) mice, which were apparently normal, were intercrossed to produce homozygous (Cas exon $2^{\Delta/\Delta}$) mutants. Cas exon $2^{\Delta/\Delta}$ mice died *in utero* at 12.5–13.5 dpc and the detailed analysis of the embryonic lethality of the Cas exon $2^{\Delta/\Delta}$ mice is underway and will be published elsewhere. In this report, we established primary fibroblasts from Cas exon 2-deficient embryos and investigated the roles of Cas exon 2 in cellular functions.

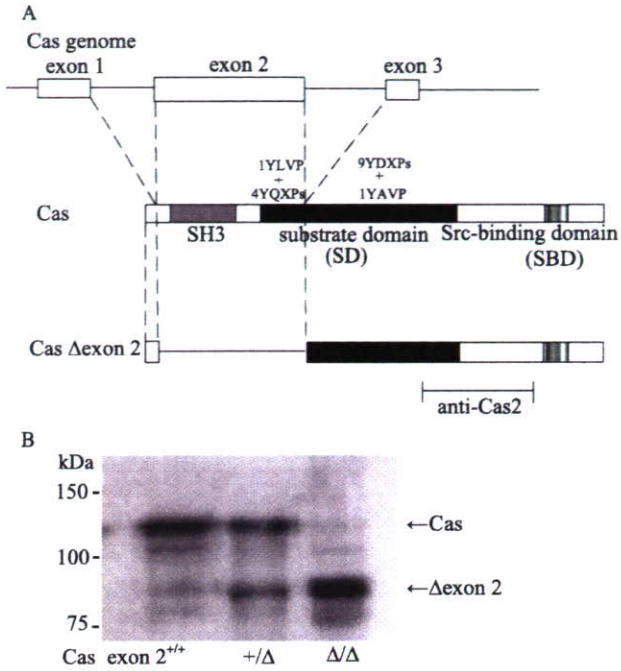

Figure 1 (A) Schematic illustration of Cas genome, Cas full-length product (Cas) and a truncated Cas protein lacking the exon 2-derived region (Cas Δexon 2). As compared to Cas, Cas Δexon 2 is deficient in the whole SH3 domain and one YLVP and four YQXP motifs. The position of the peptides for generating anti-Cas2 is also shown. (B) Western blot to detect Cas Δexon 2 protein. Thirty micrograms of cell lysates extracted from the wild-type (Cas exon $2^{+/+}$), heterozygous (Cas exon $2^{+/\Delta}$) and homozygous (Cas exon $2^{\Delta/\Delta}$) fibroblasts were separated by 7.5% SDS-PAGE, blotted to a nitrocellulose membrane and probed with 1:2000 diluted an anti-Cas antibody. Molecular weight markers are shown on the left.

Results

Cas exon $2^{\Delta/\Delta}$ cells are slower to initiate migration in the wound healing assay

To investigate functional defects caused by Cas exon 2-deficiency, we established primary fibroblasts from Cas exon 2-deficient (Cas exon $2^{\Delta/\Delta}$) embryos. Figure 1A shows the schematic diagram representing Cas Δexon 2. Cas exon 2 contains the entire SH3 domain and a part of the SD domain containing one YLVP and four YQXP motifs. It encodes 211 amino acids and the predicted molecular weight of Cas exon 2 is about 23 kDa. The expression of Cas Δexon 2 protein in Cas exon $2^{\Delta/\Delta}$ fibroblasts was detected almost as the expected size by Western blotting using an antibody against Cas, anti-Cas2 (Sakai *et al.* 1994) (Fig. 1B). Using the fibroblasts,

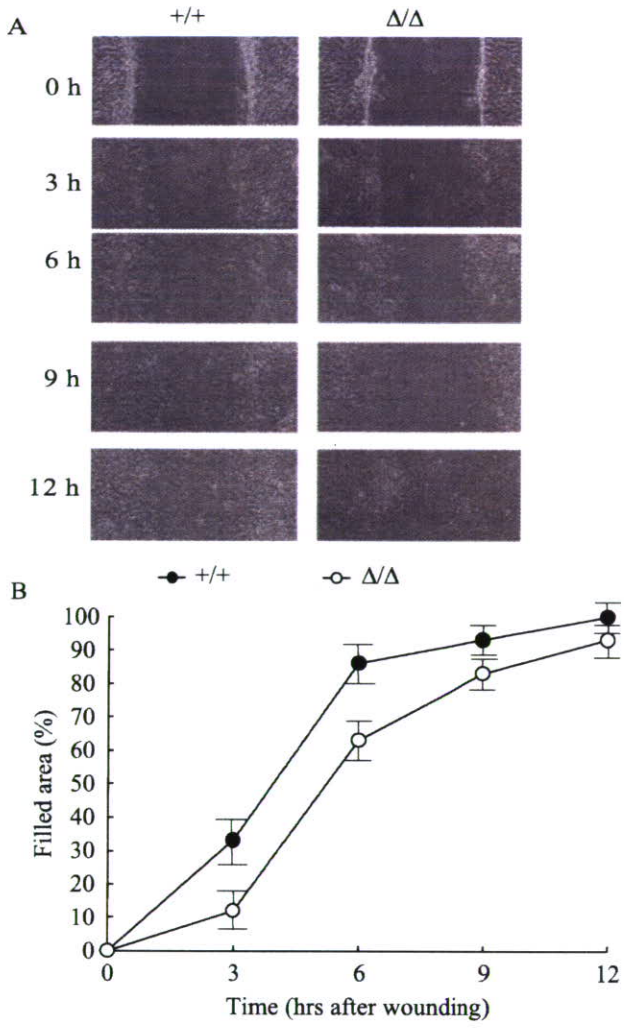

Figure 2 Delayed migration of Cas exon $2^{\Delta/\Delta}$ cells in the initial phase in the wound healing assay. (A) Photographs of Cas exon $2^{+/+}$ cells and Cas exon $2^{\Delta/\Delta}$ cells at 0, 3, 6, 9 and 12 h after wounding. Cells were first grown to confluence in plastic culture dishes, and a wound was made in the cell monolayer using a sterile micropipette tip. Cell movement was assessed 0, 3, 6, 9 and 12 h after wounding. Photographs were taken under a microscope with an objective of 100×. (B) The percentage of reduced distance between the nuclei of cells at each time period relative to the distance between two rims in the cleared field at the beginning was taken as the index (*error bars* show the standard deviation). Results presented here are representative mean values of three independent experiments.

we first performed wound healing cell migration assays. Migratory processes were assessed at 0, 3, 6, 9 and 12 h after wounding (Fig. 2A). Mean percentages of the filled area at each time points are shown in Fig. 2B. Three hours after wounding, Cas exon $2^{+/+}$ cells had filled over 30% of the gap and the cells migrating from both ends of the wound had achieved cell–cell contact. In contrast, only 10% of the area was filled by Cas exon $2^{\Delta/\Delta}$ cells. After 6 and 9 h, the migration deficit in Cas exon $2^{\Delta/\Delta}$ cells was less apparent but still present, and at 12 h the gap was almost filled in both types of the cells. This result demonstrated that Cas exon $2^{\Delta/\Delta}$ cells were deficient in ability to migrate, especially in the early phase of the response.

Cas exon $2^{\Delta/\Delta}$ cells show reduced spreading activity on fibronectin (FN)

We next examined the roles of Cas exon 2 in cell attachment, cell adhesion and cell spreading on FN. The morphological changes in Cas exon $2^{+/+}$ and Cas exon $2^{\Delta/\Delta}$ cells were observed at 30, 60 and 120 min after plating on FN-coated dishes (Fig. 3A). The mean percentages of flattened cells at each time point are shown in Fig. 3B. The disparity in cell spreading was most apparent 30 min after plating, when more than 70% of the Cas exon $2^{+/+}$ cells had already flattened, while only 37% of Cas exon $2^{\Delta/\Delta}$ cells showed a flattened phenotype. The spreading delay in Cas exon $2^{\Delta/\Delta}$ cells continued and was still observed at 120 min. These results demonstrated that Cas exon $2^{\Delta/\Delta}$ cells had a reduced ability to spread on FN.

The deficiency of Cas exon 2 impaired formation of the FAK/Cas/CrkII complex, tyrosine-phosphorylation of FAK and Cas, and FAK/Src binding on FN

Upon FN stimulation, integrin clustering promotes FAK autophosphorylation at Tyr397, which creates a binding site for the SH2 domain of Src (Mitra *et al.* 2005). FAK/Src binding leads to the conformational activation of Src and results in an activated FAK/Src signaling complex (Schlaepfer *et al.* 2004), which enhances tyrosine-phosphorylation of Cas (Sakai *et al.* 1994; Mitra *et al.* 2005) Tyrosine-phosphorylated Cas binds to CrkII through the SD domain with preference for YDXP motifs (Songyang *et al.* 1993), which subsequently leads to activate downstream small GTP-binding proteins through C3G (Kiyokawa *et al.* 1998a,b; Klemke *et al.* 1998) and plays a key role in cell migration (Fig. 8A).

We then investigated whether the deficiency of Cas exon 2 might affect Cas' association with its major signaling molecules, FAK (Polte & Hanks 1995), Src (Nakamoto *et al.* 1996) and CrkII (Mayer *et al.* 1995) to which Cas binds through its SH3, SBD and SD, respectively. Protein aliquots extracted from Cas exon $2^{+/+}$ and

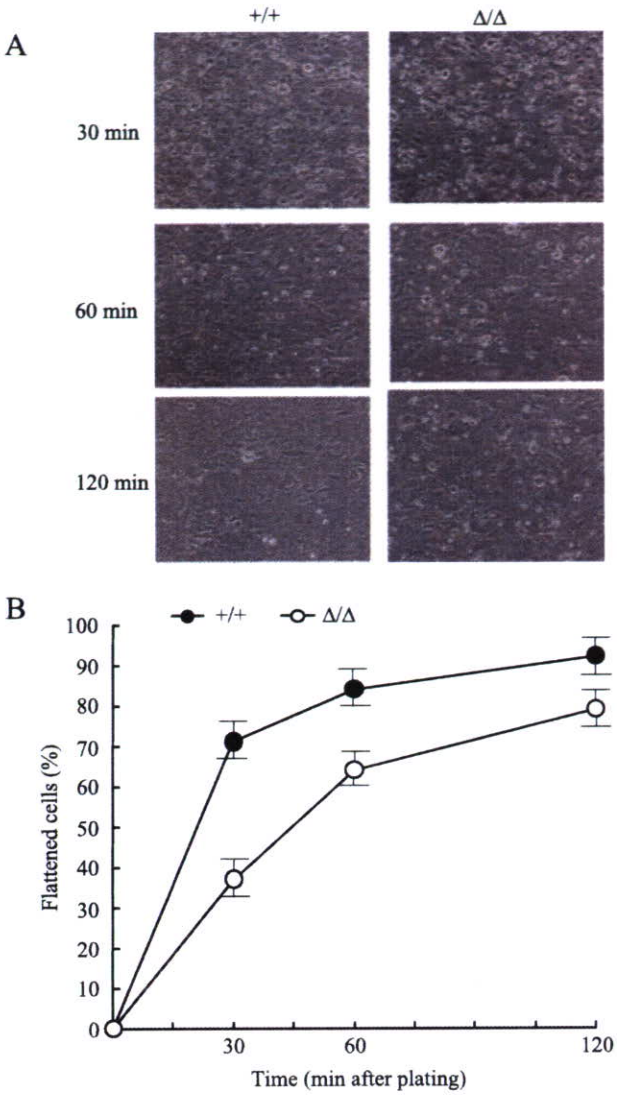

Figure 3 Reduced spreading ability of Cas exon $2^{\Delta/\Delta}$ cells on FN. (A) Photographs of Cas exon $2^{+/+}$ cells and Cas exon $2^{\Delta/\Delta}$ cells at 30, 60 and 120 min after plating on FN-coated dishes. Cells were added to FN-coated dishes and incubated at 37 °C for indicated times. Photographs were taken under a microscope with an objective of 100×. (B) Cell spreading was quantitated by calculating the percentages of spread cells (*error bars* show the standard deviation). Single cells that were phase-bright with rounded morphology were scored non-spread, whereas those that possessed a flattened shape and looked phase-dark were scored as spread. Results presented here are representative mean values of eight independent fields of three experiments.

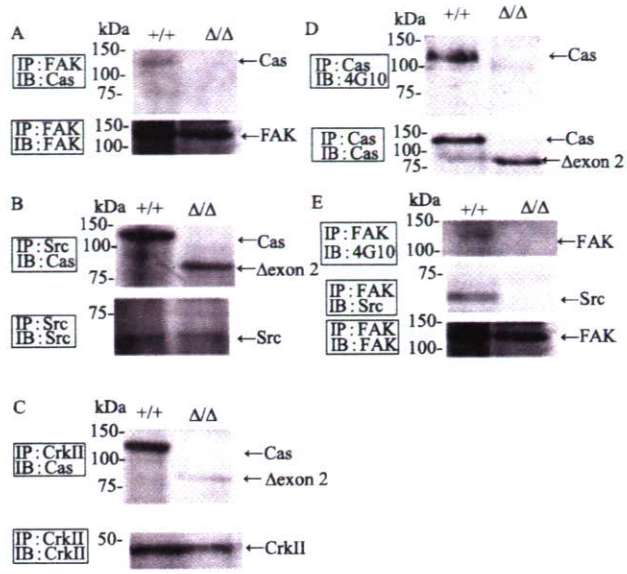

Figure 4 Impaired FAK/Cas/CrkII complex formation, tyrosine-phosphorylation of FAK and Cas, and FAK/Src binding upon FN stimulation in Cas exon $2^{\Delta/\Delta}$ cells. Serum-starved Cas exon $2^{+/+}$ cells and Cas exon $2^{\Delta/\Delta}$ cells were cultured on FN-coated dishes for 1 h, harvested and lysed with 1% Triton lysis buffer. (A) FAK immunoprecipitates (IP : FAK) were probed with anti-Cas (IB : Cas) or anti-FAK (IB : FAK). (B) Src immunoprecipitates (IP : Src) were probed with anti-Cas (IB : Cas) or anti-Src (IB : Src). (C) CrkII immunoprecipitates (IP : CrkII) were probed with anti-Cas (IB : Cas) or anti-CrkII (IB : CrkII). (D) Cas immunoprecipitates (IP : Cas) were probed with 4G10 (IB : 4G10) or anti-Cas (IB : Cas). (E) FAK immunoprecipitates (IP : FAK) were probed with 4G10 (IB : 4G10), anti-Src (IB : Src) or anti-FAK (IB : FAK).

Cas exon $2^{\Delta/\Delta}$ cells plated on FN were immunoprecipitated with antibodies against either FAK, Src or CrkII and immunoprecipitated proteins were blotted with anti-Cas2. As shown in Fig. 4A, wild-type Cas was associated with FAK, whereas Cas Δexon 2 could not bind to FAK. By contrast, Fig. 4B shows that Src bound to both Cas and Cas Δexon 2 at similar levels. We then analyzed possible alteration in CrkII binding to Cas in Cas exon $2^{\Delta/\Delta}$ cells. As shown in Fig. 4C, in Cas exon $2^{+/+}$ cells, stable complex formation of Cas and CrkII was detected, whereas in Cas exon $2^{\Delta/\Delta}$ cells, the binding activity of CrkII to Cas Δexon 2 was significantly reduced. We then analyzed whether the deficiency of Cas exon 2 might affect tyrosine-phosphorylation of Cas. As shown in Fig. 4D, Cas Δexon 2 was not tyrosine-phosphorylated upon FN stimulation. In addition, we could not detect FAK tyrosine-phosphorylation and FAK/Src binding (Fig. 4E). These results indicated that Cas exon 2-deficiency impaired formation of the FAK/Cas/CrkII complex, tyrosine-phosphorylation of FAK and Cas, and FAK/Src binding upon FN stimulation.

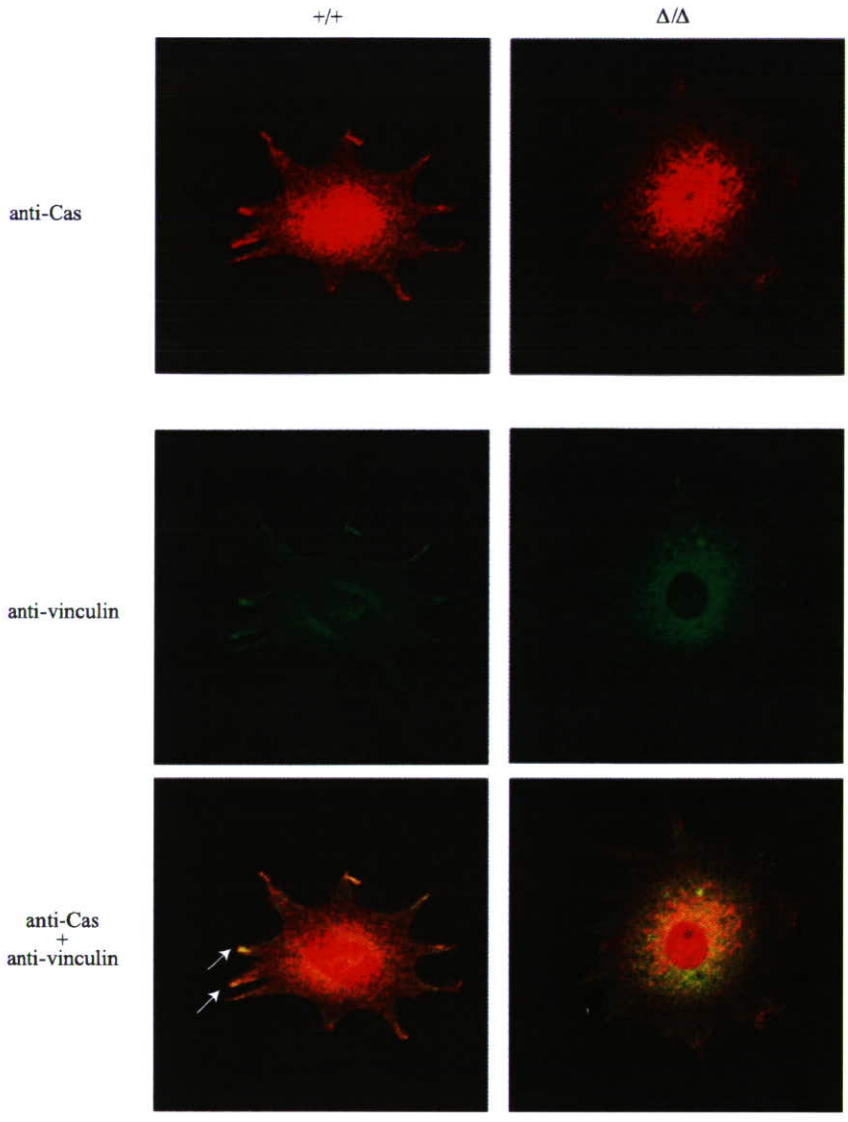

Figure 5 Cas exon 2 is required for the localization of Cas to focal adhesions upon FN stimulation. Cas exon $2^{+/+}$ and Cas exon $2^{\Delta/\Delta}$ cells grown on FN-coated coverslips were stained with anti-Cas and anti-vinculin (hVIN-1) antibodies. Texas red-labeled secondary antibody targeted the anti-Cas antibody and Fluorescein-labeled secondary antibody labeled the anti-vinculin antibody. Following FN stimulation, wild-type Cas was recruited to focal adhesions, as demonstrated by the yellow double staining pattern (left lower panel, indicated by *arrows*), whereas Cas Δexon 2 remained in the cytoplasm and did not concentrate at focal adhesions (right lower panel).

Cas exon 2 is required for the localization of Cas to focal adhesions upon FN stimulation

We compared the subcellular localization of wild-type Cas and Cas Δexon 2 in primary fibroblasts stimulated by FN. Cas exon $2^{+/+}$ and Cas exon $2^{\Delta/\Delta}$ cells grown on FN-coated coverslips were stained with an anti-Cas2. Anti-vinculin (hVIN-1) staining was also performed to identify focal adhesions. As shown in Fig. 5, following FN stimulation, wild-type Cas was recruited to focal adhesions as previously reported (Nakamoto *et al.* 1997), as demonstrated by the yellow double staining pattern (Fig. 5, left lower panel, indicated by *arrows*), whereas Cas Δexon 2 was retained mainly in the cytoplasm and was not concentrated at focal adhesions (Fig. 5, right lower panel). The results indicated that Cas exon 2 is required for the localization of Cas to focal adhesions upon FN stimulation.

The deficiency of Cas exon 2 up-regulated cell adhesion-associated genes including CXC Chemokine Receptor-4 (CXCR4), CC Chemokine Receptor-5 (CCR5) and thrombospondin 4 in primary fibroblasts

To further characterize the role of Cas exon 2 in intracellular signaling, we performed microarray analyses to investigate alterations in gene expression caused by Cas exon 2-deficiency. RNA samples extracted from Cas exon $2^{+/+}$, Cas exon $2^{+/\Delta}$ and Cas exon $2^{\Delta/\Delta}$ fibroblasts

(12.5 dpc, two embryos for each genotype) were subjected to microarray analysis as described in Experimental procedures. Gene expression patterns of Cas exon $2^{\Delta/\Delta}$ fibroblasts were compared with those of Cas exon $2^{+/+}$ and Cas exon $2^{+/\Delta}$ cells. The complete microarray data set is available from the gene expression omnibus (GEO) database (accession no. GSE8357). Expressed sequence tags were excluded and genes that showed more than a 3.0-fold change in expression are presented in Table 1. One interesting aspect of the result is that cell migration- and cell adhesion-associated genes, such as chemokine ligands/receptors and thrombospondin, were listed among the genes up-regulated by Cas exon 2-deficiency. We thus confirmed the up-regulation of these genes in Cas exon $2^{\Delta/\Delta}$ fibroblasts by quantitative real-time RT-PCR analysis. The results showed that the expression levels of three genes, CXCR4, CCR5 and thrombospondin 4, were significantly enhanced by Cas exon 2-deficiency. The changes in expression measured by microarray analysis correlated well with data from quantitative real-time RT-PCR analyses (Fig. 6). These results demonstrated that the loss of Cas exon 2 induced expression of CXCR4, CCR5 and thrombospondin 4, genes involved in cell motility in primary fibroblasts.

Phospho-IκBα level was augmented in Cas exon $2^{\Delta/\Delta}$ fibroblasts

We then examined the underlying molecular mechanism for the up-regulated expression of CXCR4 and CCR5 in Cas exon $2^{\Delta/\Delta}$ fibroblasts. It is already demonstrated that the extracellular signal-activated transcription factor nuclear factor-κB (NF-κB) regulates the expression of some chemokine ligands/receptors, including CXCR4 (Helbig *et al.* 2003; Kukreja *et al.* 2005) and CCR5 (Kim *et al.* 2006). Activation of NF-κB requires phosphorylation of IκBα. Thus, we compared phospho-IκBα levels between Cas exon $2^{+/+}$ and Cas exon $2^{\Delta/\Delta}$ fibroblasts. As shown in Fig. 7, the phosphorylation level of IκBα was significantly augmented in Cas exon $2^{\Delta/\Delta}$ cells as compared to Cas exon $2^{+/+}$ cells. These results indicated that that the NF-κB signaling pathway was activated by Cas exon 2 deficiency, which would play a role in up-regulated expression of CXCR4 and CCR5 in Cas exon $2^{\Delta/\Delta}$ fibroblasts.

Discussion

Cas is an adaptor molecule implicated in various biological processes, such as cell adhesion, cell migration, cell apoptosis, cell transformation and bacterial infection (Defilippi *et al.* 2006). Structurally, Cas is an adaptor

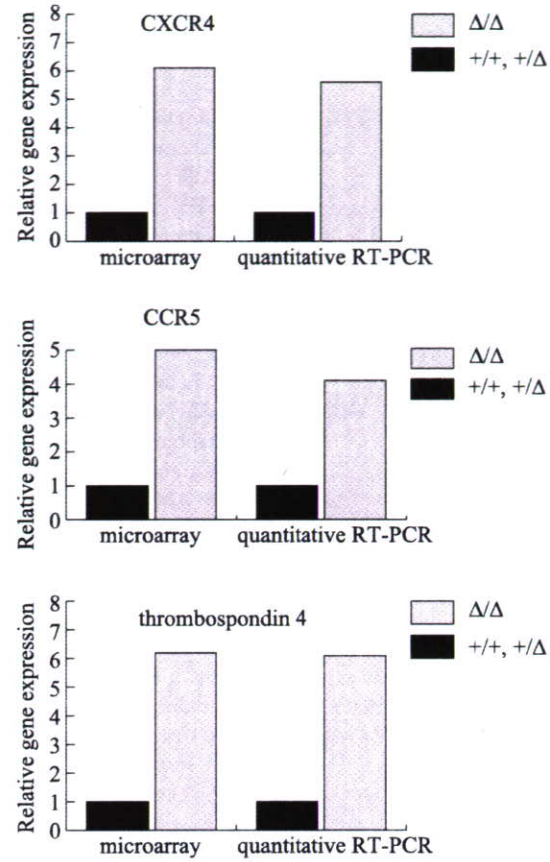

Figure 6 Up-regulated expression of CXCR4, CCR5 and thrombospondin 4 in Cas exon $2^{\Delta/\Delta}$ fibroblasts. RNA samples extracted from Cas exon $2^{+/+}$, Cas exon $2^{+/\Delta}$ and Cas exon $2^{\Delta/\Delta}$ fibroblasts (12.5 dpc, three embryos for each genotype) were used. The changes in expression levels determined by microarray (left) or quantitative real-time RT-PCR (right) are shown.

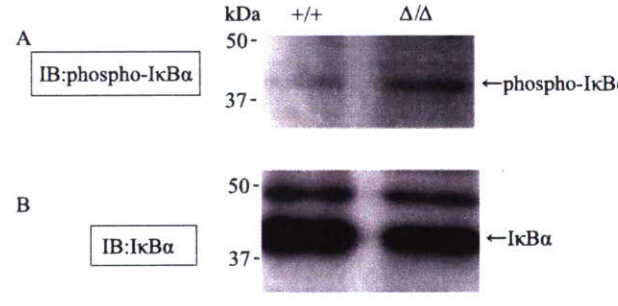

Figure 7 Increased phosphorylation of IκBα in Cas exon $2^{\Delta/\Delta}$ fibroblasts. Cas exon $2^{+/+}$ cells and Cas exon $2^{\Delta/\Delta}$ cells were harvested and lysed with 1% Triton lysis buffer. Equal amounts of total cell lysates were blotted with anti-phospho-IκBα (A) or an anti-IκBα (B).

Table 1 (A) Genes up-regulated in Cas exon $2^{\Delta/\Delta}$ fibroblasts

Fold change	Description	UniGene
46.72	Jumonji, AT rich interactive domain 1D (Rbp2 like)	Mm.262676
12.8	Chemokine (C–C motif) ligand 12	Mm.867
11.2	Killer cell lectin-like receptor, subfamily A, member 2	Mm.4783
7.812	SPARC-like 1 (mast9, hevin)	Mm.29027
6.172	Thrombospondin 4	Mm.20865
6.06	Chemokine (C–C motif) receptor 5	Mm.14302
5.988	Astrotactin 1	Mm.329586
5.714	EGF-like-domain, multiple 6	Mm.37707
5.263	Chemokine (C–C motif) ligand 3	Mm.1282
5.102	Chemokine (C–C motif) ligand 9	Mm.2271
5.025	Chemokine (C–X–C motif) receptor 4	Mm.1401
4.484	Lipoprotein lipase	Mm.1514
4.444	Carbonic anhydrase 2	Mm.1186
4.405	SLAM family member 7	Mm.164642
4.405	RAS-like, estrogen-regulated, growth-inhibitor	Mm.46233
4.149	Macrophage scavenger receptor 1	Mm.239291
4	Odd-skipped related 2 (*Drosophila*)	Mm.46336
3.984	X-linked lymphocyte-regulated 3a	Mm.195091
3.921	C-type lectin domain family 14, member a	Mm.280563
3.831	Schlafen 8	Mm.347694
3.802	Interferon activated gene 203	Mm.261270
3.623	G-protein coupled receptor 65	Mm.378924
3.584	Hepatitis A virus cellular receptor 2	Mm.72168
3.571	Sciellin	Mm.244003
3.333	Adrenomedullin receptor	Mm.2857
3.257	Matrix metalloproteinase 12	Mm.2055
3.236	Cytochrome b-245, β polypeptide	Mm.200362
3.205	Interferon, α-inducible protein 27	Mm.271275
3.195	Prostaglandin E receptor 2 (subtype EP2)	Mm.4630
3.185	Mannose receptor, C type 1	Mm.2019
3.175	Complement component 2 (within H-2S)	Mm.283217
3.155	C-type lectin domain family 4, member d	Mm.299633
3.115	Disabled homolog 2 (*Drosophila*)	Mm.240830

(B) Genes down-regulated in Cas exon $2^{\Delta/\Delta}$ fibroblasts

Fold change	Description	UniGene
−14.19	Xlr-related, meiosis regulated	Mm.14300
−14.17	Kallikrein 24	Mm.378954
−8.397	RIKEN cDNA E130012A19 gene	Mm.24506
−7.892	Vomeronasal 1 receptor, D7	Mm.160377
−7.051	RIKEN cDNA 4933413N12 gene	Mm.158581
−6.949	Probasin	Mm.8034
−6.489	Fibroblast growth factor 16	Mm.154768
−6.432	Phosphatidylinositol glycan, class H	Mm.281044
−5.785	Interleukin-1 receptor-associated kinase 4	Mm.279655
−5.717	RIKEN cDNA 4921517J23 gene	Mm.291129
−5.645	Forkhead box A1	Mm.4578
−5.54	RIKEN cDNA 4931406I20 gene	Mm.318331
−5.344	Phosphatase, orphan 1	Mm.133075
−5.058	RIKEN cDNA 1700020N01 gene	Mm.54306
−5.029	myosin, heavy polypeptide 1, skeletal muscle	Mm.340118

Continued overleaf

Table 1 *Continued*

Fold change	Description	UniGene
−4.676	Thyrotropin releasing hormone receptor	Mm.309350
−4.635	Elongation protein 4 homolog (*S. cerevisiae*)	Mm.33870
−4.213	Leukotriene A4 hydrolase	Mm.271071
−4.191	Serine dehydratase-like	Mm.5162
−4.171	Actin related protein M2	Mm.30958
−4.135	Component of Sp100-rs	Mm.362648
−4.058	RIKEN cDNA C230093N12 gene	Mm.4065
−3.843	Procollagen, type II, α1	Mm.2423
−3.734	Calcitonin receptor-like	Mm.75467
−3.528	SRY-box containing gene 10	Mm.276739
−3.46	Profilin 3	Mm.348015
−3.436	Defensin β7	Mm.207067
−3.329	Titin-cap	Mm.10762
−3.329	Melanocortin 3 receptor	Mm.57183
−3.311	Flavin containing monooxygenase 1	Mm.976
−3.271	RIKEN cDNA 2410017P07 gene	Mm.338605
−3.231	Transketolase-like 1	Mm.25057
−3.216	Expressed sequence AU041707	Mm.200898
−3.211	Chromobox homolog 1 (*Drosophila* HP1 β)	Mm.29055
−3.104	Deleted in azoospermia-like	Mm.280641
−3.045	Forkhead box G1	Mm.4704

molecule composed of SH3, SD and SBD (Fig. 1A), and exerts its biological function by interacting various intracellular molecules, such as FAK, CrkII and Src, through its different functional domains. In this paper, to primarily focus on the role of Cas SH3 in cellular function, we established and analyzed primary fibroblasts from mice that were engineered to produce truncated Cas lacking the exon 2-derived region containing the whole SH3 domain (Cas Δexon 2).

As expected from a previous study (Polte & Hanks 1995), we demonstrated that Cas Δexon 2 lost its ability to bind to FAK but retained the ability to bind to Src, irrespective of FN stimulation (Fig. 4A and B and data not shown). In addition, we found that upon FN stimulation, the binding activity of Cas Δexon 2 to CrkII was significantly reduced (Fig. 4C). This result seems curious since the YDXP motifs in the SD, that are the preferred binding site to the CrkII SH2 domain when phosphorylated (Songyang *et al.* 1993), are all conserved in Cas Δexon 2. To investigate the underlying mechanism, we analyzed tyrosine-phosphorylation of Cas between two types of cells. Upon FN stimulation, Cas was apparently tyrosine-phosphorylated in Cas exon $2^{+/+}$ cells as previously reported (Nojima *et al.* 1995), whereas we could not detect tyrosine-phosphorylation of Cas Δexon 2 in Cas exon $2^{\Delta/\Delta}$ cells (Fig. 4D). In addition, we examined tyrosine-phosphorylation of FAK, which is the primary event following integrin stimulation. Surprisingly, FAK was not tyrosine-phosphorylated in Cas exon $2^{\Delta/\Delta}$ cells (Fig. 4E). Furthermore, FAK/Src binding was not detected in Cas exon $2^{\Delta/\Delta}$ cells (Fig. 4E), probably owing to impaired tyrosine-phosphorylation of FAK. These results indicate that Cas exon 2 is essential for FAK auto-phosphorylation upon FN. This idea is in line with a previous study, in which Cas lacking SH3 failed to bind to CrkII, which subsequently abolished FAK/Cas/CrkII complex formation as well as FAK auto-phosphorylation by FN (Iwahara *et al.* 2004). The underlying mechanism for impaired tyrosine-phosphorylation of FAK in Cas exon $2^{\Delta/\Delta}$ cells remains unclear. One possibility is that the constitutive FAK/Cas binding might be essential for conformational change of FAK tyrosine-phosphorylation. Alternatively, the FAK/Cas complex formation might be required for FAK to keep the tyrosine-phosphorylated state. A previous study showed that CrkII knockdown reduces integrin-stimulated FAK Tyr397 autophosphorylation (Iwahara *et al.* 2004). Therefore, the Cas/CrkII complex may also affect tyrosine-phosphorylation of FAK as an upstream regulator in reverse (Iwahara *et al.* 2004).

We also compared the intracellular localization of Cas and Cas Δexon 2 upon FN stimulation. In contrast to Cas to be localized to focal adhesions as previously reported (Nakamoto *et al.* 1997), no clear localization of

Cas Δexon 2 at focal adhesions was found (Fig. 5). Impaired recruitment of Cas to focal adhesions following FN stimulation was reported in Src-deficient cells (Nakamoto *et al.* 1997), and Src can be regarded as a recruiting molecule of Cas to focal adhesions (Kaplan *et al.* 1995; Honda *et al.* 1999). Although Cas Δexon 2 and wild-type Cas have comparable binding abilities to bind Src (Fig. 4B), Cas Δexon 2 was not found in focal adhesions (Fig. 5), indicating that Cas exon 2 plays an essential role in the localization of Cas to focal adhesions upon FN stimulation. This idea is supported by our previous finding that Cas lacking SH3 failed to localize at focal adhesions on FN stimulation when expressed in COS-7 cells (Nakamoto *et al.* 1997). While the mechanism is not clear, one possibility is that when Cas Δexon 2 is recruited to focal adhesions by Src, FAK is not tyrosine-phosphorylated and cannot bind to Cas Δexon 2 and Src, which in turn would allow release of Cas Δexon 2 from focal adhesions. Another possibility is that the impaired FAK/Src complex leads to reduced activation of Src, which could not recruit Cas Δexon 2 to focal adhesions. It is possible that impaired tyrosine-phosphorylation of FAK and Cas leads to incomplete formation of FAK/Cas/Src/CrkII complex and impaired localization of Cas to focal adhesions, which resulted in delayed cell migration (Fig. 2) and spreading on FN (Fig. 3). A previous study using the Cas SD mutants and examining their ability to heal the wound revealed that the effective wound healing was achieved by Cas variants containing at least four of the YDXP/YAVP motifs, the major phosphorylation sites of Cas SD (Shin *et al.* 2004). Since YDXP/YAVP motifs, which serve main binding sites to CrkII, are all conserved in Cas exon $2^{\Delta/\Delta}$ cells (see Fig. 1A), it would be unlikely that the reduced motility is due to the lack of YLVP/YQXP motifs existing in exon 2. In addition, we found that the defects observed in Cas exon $2^{\Delta/\Delta}$ cells were less apparent than those in $Cas^{-/-}$ cells (Honda *et al.* 1999). The reason might be that since Cas exon $2^{\Delta/\Delta}$ cells retain the YDXP/YAVP motifs and the SBD as compared to $Cas^{-/-}$ cells, these domains would partly participate in downstream signaling. In fact, a slight amount of CrkII could bind to Cas upon FN stimulation (Fig. 4C).

To identify downstream molecules regulated by Cas exon 2, we investigated the expression profile of Cas exon $2^{\Delta/\Delta}$ fibroblasts using microarray methods (Table 1). Interestingly, we found that cell migration- and cell adhesion-associated genes, such as chemokine ligands/receptors and thrombospondin, were up-regulated by Cas exon 2 deficiency. We previously compared the expression profile of $Cas^{-/-}$ fibroblasts with that in Cas-re-expressing fibroblasts using the same methods (Nakamoto *et al.* 2002), but could not detect changes in expression of chemokine ligands/receptors and thrombospondins. Thus, the expression changes in these genes (chemokine ligands/receptors and thrombospondins) may be specifically regulated by Cas exon 2-mediated signals.

We also demonstrated that the phospho-IκBα level was augmented in Cas exon $2^{\Delta/\Delta}$ cells, indicating that the NF-κB signaling pathway was activated by Cas exon 2 deficiency (Fig. 7). Based on this result, it is conceivable that up-regulated expression of CXCR4 and CCR5 in Cas exon $2^{\Delta/\Delta}$ fibroblasts is, at least in part, dependent on IκBα phosphorylation. The mechanism underlying the activation of NF-κB signaling and up-regulated expression of CXCR4 and CCR5 is not clear. One possibility is that since the 5′-promoter region of FAK contains NF-κB binding sites, the NF-κB transcription factor might play a role in regulating FAK transcription (Golubovskaya *et al.* 2004). It would also be possible that NF-κB is activated to compensate for the impaired tyrosine-phosphorylation of FAK and FAK/Cas binding in Cas exon $2^{\Delta/\Delta}$ cells.

In summary, we demonstrated that Cas exon 2 plays an essential role in cell migration, cell spreading on FN, tyrosine-phosphorylation of FAK and Cas, FAK/Cas/Src/CrkII complex formation and recruitment of Cas to focal adhesions in primary fibroblasts. In addition, we showed that Cas exon 2-deficiency significantly up-regulated expression of CXCR4 and CCR5, molecules implicated in cell motility (Fig. 8). Our findings define the biological roles of Cas exon 2 and provide novel insights into Cas SH3 function in intracellular signaling.

Experimental procedures

Antibodies

A polyclonal antibody against Cas, anti-Cas2, was generated as previously described (Sakai *et al.* 1994). Antibodies against FAK, Src and CrkII were from Santa Cruz Biotechnology, Santa Cruz, CA, anti-phosphotyrosine antibody 4G10 was from Upstate Biotechnology, Lake Placid, NY and hVIN-1 was from Sigma, St. Louis, MO. Anti-IκBα and anti-phospho-IκBα were from Cell Signaling Technology, Danvers, MA. Anti-Fluorescein-labeled and Texas red-labeled secondary antibodies were from Invitrogen, Carlsbad, CA.

Cultivation of primary fibroblasts

Cas exon $2^{+/\Delta}$ mice were intercrossed and embryos at 12.5 dpc were collected. Heads and internal organs were used for genotyping and primary embryonic fibroblasts were isolated from the remaining of embryos and cultured in Dulbecco's modified Eagle's